Article

Immunity

The Intestinal Microbiota Contributes to the Ability of Helminths to Modulate Allergic Inflammation

Highlights

- The microbiota contributes to helminth-induced modulation of allergic asthma
- Cecal microbial communities are altered in helminth-infected mice
- Helminth infection increases microbial-derived short chain fatty acids
- GPR41 mediates helminth-induced Treg cell suppressor function

Authors

Mario M. Zaiss, Alexis Rapin, Luc Lebon, ..., Tobias Junt, Benjamin J. Marsland, Nicola L. Harris

Correspondence

nicola.harris@epfl.ch

In Brief

Intestinal helminths are well known to possess potent immunomodulatory capacities. Harris and colleagues demonstrate in mice that helminth infection alters the bacterial microbiota and increases the concentration of short chain fatty acids (SCFAs), which reduce allergic asthma via GPR41. Increased intestinal SCFA concentrations were conserved across multiple parasite and host species.

Zaiss et al., 2015, Immunity *43*, 998–1010
November 17, 2015
http://dx.doi.org/10.1016/j.immuni.2015.09.012

CellPress

CellPress

Immunity
Article

The Intestinal Microbiota Contributes to the Ability of Helminths to Modulate Allergic Inflammation

Mario M. Zaiss,[1] Alexis Rapin,[1] Luc Lebon,[1] Lalit Kumar Dubey,[1] Ilaria Mosconi,[1] Kerstin Sarter,[2] Alessandra Piersigilli,[1,3] Laure Menin,[4] Alan W. Walker,[5,6] Jacques Rougemont,[7] Oonagh Paerewijck,[8] Peter Geldhof,[8] Kathleen D. McCoy,[9] Andrew J. Macpherson,[9] John Croese,[10,11] Paul R. Giacomin,[11] Alex Loukas,[11] Tobias Junt,[12] Benjamin J. Marsland,[13] and Nicola L. Harris[1,*]

[1]Global Health Institute, École Polytechnique Fédérale de Lausanne (EPFL), Lausanne 1015, Switzerland
[2]Department of Pathology and Immunology, Faculty of Medicine, University of Geneva, Geneva 1211, Switzerland
[3]Institute of Animal Pathology, Vetsuisse Faculty, University of Bern, Bern 3012, Switzerland
[4]Institute of Chemical Sciences and Engineering, École Polytechnique Fédérale de Lausanne (EPFL), Lausanne 1015, Switzerland
[5]Pathogen Genomics Group, Wellcome Trust Sanger Institute, Hinxton, Cambridgeshire CB10 1SA, UK
[6]Microbiology Group, Rowett Institute of Nutrition and Health, University of Aberdeen, Aberdeen AB21 9SB, UK
[7]Bioinformatics and Biostatistics Core Facility, École Polytechnique Fédérale de Lausanne (EPFL) and Swiss Institute of Bioinformatics, Lausanne 1015, Switzerland
[8]Department of Virology, Parasitology and Immunology, Ghent University, Salisburylaan 133, 9820 Merelbeke, Belgium
[9]Maurice Müller Laboratories (DKF), University Hospital of Bern, Bern 3010, Switzerland
[10]Department of Gastroenterology and Hepatology, The Prince Charles Hospital, Chermside, Brisbane, QLD 4032, Australia
[11]Australian Institute of Tropical Health and Medicine, James Cook University, Cairns, QLD 4870, Australia
[12]Novartis Pharma AG, Basel 4056, Switzerland
[13]Faculty of Biology and Medicine, University of Lausanne, Centre Hospitalier Universitaire Vaudois (CHUV), Lausanne 1011, Switzerland
*Correspondence: nicola.harris@epfl.ch
http://dx.doi.org/10.1016/j.immuni.2015.09.012

SUMMARY

Intestinal helminths are potent regulators of their host's immune system and can ameliorate inflammatory diseases such as allergic asthma. In the present study we have assessed whether this anti-inflammatory activity was purely intrinsic to helminths, or whether it also involved crosstalk with the local microbiota. We report that chronic infection with the murine helminth *Heligmosomoides polygyrus bakeri* (Hpb) altered the intestinal habitat, allowing increased short chain fatty acid (SCFA) production. Transfer of the Hpb-modified microbiota alone was sufficient to mediate protection against allergic asthma. The helminth-induced anti-inflammatory cytokine secretion and regulatory T cell suppressor activity that mediated the protection required the G protein-coupled receptor (GPR)-41. A similar alteration in the metabolic potential of intestinal bacterial communities was observed with diverse parasitic and host species, suggesting that this represents an evolutionary conserved mechanism of host-microbe-helminth interactions.

INTRODUCTION

Intestinal helminths have co-evolved together with their mammalian hosts over several hundred million years (Gause et al., 2013). Although these organisms have been virtually eradicated within industrialized countries, approximately 2 billion people, mainly children from areas without adequate sanitation, suffer from chronic intestinal helminth infections and associated morbidity (Hotez et al., 2014). To ensure their long-term survival, helminths have evolved potent mechanisms to regulate the host immune response (Maizels et al., 2004). Indeed, together with increased sanitary standards, the eradication of intestinal helminths from industrialized countries has been proposed to contribute to the increased incidence of immune-mediated disorders apparent in these regions (Maizels and Yazdanbakhsh, 2003). Epidemiological evidence supports this view with studies showing a negative correlation between helminth infection and allergen skin test reactivity (Cooper et al., 2003). Experimental helminth infection can limit disease severity in murine models of arthritis (Salinas-Carmona et al., 2009), type 1 diabetes (Mishra et al., 2013; Osada et al., 2013), colitis (Weinstock, 2006), and allergic airway inflammation (Wilson et al., 2005). Such findings have heightened interest in the use of these parasites, or their secreted products, for the treatment of inflammatory diseases. Consequently, live helminths are currently employed in at least 15 clinical trials in efforts to alleviate allergic and autoimmune disorders (Khan and Fallon, 2013).

The exact mechanisms behind the potent immuno-modulatory capacity of helminths remain largely unknown. Numerous species secrete anti-inflammatory products, a few of which have been characterized (Maizels et al., 2004). Moreover, data indicate that intestinal helminth infections also impact the composition of the gut microbiota (Broadhurst et al., 2012; Osborne et al., 2014; Rausch et al., 2013; Walk et al., 2010; Wu et al., 2012), raising the possibility that these organisms might

exert immuno-modulatory activity in an indirect manner as well. Helminth-induced alterations to the gut microbiota are of particular interest because this diverse and complex community can have a profound impact on host homeostasis and the development of immune-mediated diseases (Macpherson and Harris, 2004). Changes in the gut microbiota through the use of antibiotics, particularly during infancy or childhood, have been correlated with the occurrence of allergic disease, multiple sclerosis, and inflammatory bowel disease (IBD) in humans (Zeissig and Blumberg, 2014). These findings are further supported by experimental studies showing that mice lacking intestinal bacteria (germ-free mice) exhibit increased allergy (Herbst et al., 2011) and that susceptibility to obesity or IBD can be transferred together with the intestinal microbiota (Garrett et al., 2007; Turnbaugh et al., 2008). The means by which intestinal bacteria impact our health are likely to be varied and complex, and it is increasingly appreciated that the vast array of metabolites produced by the intestinal microbiota might interact closely with our immune system to create a microbial-metabolite-immune axis (Dorrestein et al., 2014).

In the current study we explored the possibility that intestinal helminths modulate allergic diseases, at least in part, through alterations to the microbiota of the intestine. Our findings show that murine intestinal helminth infection not only alters the intestinal bacterial communities but that intestinal bacteria contribute to the ability of helminth infection to attenuate allergic airway inflammation. The immuno-modulatory capacity of helminth infection could be transferred through fecal transplantation and correlated with an increased availability of microbial-derived short chain fatty acids (SCFAs). A direct link between helminth-induced increases in SCFAs and the ability of these organisms to attenuate allergic airway inflammation was shown using mice lacking the SCFA cognate receptor GPR41 (also called free fatty acid receptor 3 [FFAR3]). These data indicate that helminths not only modulate the immune system directly, but that they also impact allergic airway disease by increasing bacterial-derived immuno-modulatory metabolites.

RESULTS

Intestinal Helminth Infection Can Reduce the Severity of Allergic Airway Inflammation

Several studies have demonstrated that *Heligmosomoides polygyrus bakeri* (Hbp) infection can attenuate the development of allergic airway disease in mice sensitized with model antigens via the intra-peritoneal route (McSorley et al., 2012; Wilson et al., 2005). To determine whether Hpb infection could also attenuate airway inflammation by a more physiological regime, we exposed naive or Hpb-infected specific-pathogen-free (SPF) mice to house dust mite (HDM) extracts via the intranasal route three times per week for 3 consecutive weeks. Helminth infection attenuated the allergic inflammation as evidenced by a specific reduction in the total number (Figure 1A) and percentage (Figure 1B) of infiltrating eosinophils. This decreased eosinophilia correlated with a reduced presence of type 2 cell-associated cytokines in the airways (Figures 1C and 1D) and reduced HDM-specific IgG1 (Figure 1E). Infection did not impact airway hyper-reactivity (AHR), as measured by increased airway resistance after methacholine challenge (Figure 1F). However, we did note a decline in inflammatory cells infiltrating the lung tissue (Figure 1G), together with decreased goblet cell hyperplasia (Figure 1H), indicating a significant reduction in allergen-induced pathology.

Intestinal Bacteria Contribute to the Ability of Helminths to Attenuate Allergic Airway Inflammation

To address whether the modulation of allergic airway inflammation by chronic helminth infection required the presence of intestinal bacteria, we infected antibiotic-treated mice. The antibiotic treatment eliminated bacteria by a factor of 10^5–10^6 for aerobic and 10^6–10^7 for anaerobic bacteria (Figures S1A and S1B). In addition, no fungal outgrowth was detected. Mice were then challenged with HDM and the ensuing inflammatory response analyzed. As expected, helminth infection of SPF mice resulted in a reduced number (Figure 2A) and proportion (Figure 2B) of infiltrating eosinophils. Type 2 cell-associated cytokine concentration in the airways (Figures 2C and 2D) and HDM-specific IgG1 (Figure 2E) were also reduced in helminth-infected SPF mice. Notably, helminth infection did not attenuate the severity of inflammation in antibiotic-treated mice (Figures 2A–2E), even though adult worm numbers were comparable to SPF mice (Figure S1C). These data indicate that the host microbiota is required for Hpb-mediated modulation of the allergic response.

We next assessed whether re-colonization of antibiotic-treated mice with a microbiota from Hpb-infected mice via co-housing was sufficient to confer protection. Naive SPF, or Hpb-infected SPF, donor mice were co-housed with antibiotic-treated recipients for a period of 3 weeks. Of note, such co-housing allowed the transfer only of the bacterial microbiota and not of the parasite, because adult worms cannot replicate within their hosts nor can they infect new hosts. As a control, recipient mice were monitored for the presence of live worms at the time of sacrifice with no Hpb worms being detected (Figure S1D). Co-housing was followed by an exposure of all recipient mice to HDM. Recipient mice co-housed with helminth-infected donors exhibited a reduced number and proportion of airway eosinophils (Figures 2F and 2G) compared to recipients co-housed with naive donors. These changes were paralleled by reductions in HDM-specific IgG1 (Figure 2H), lung pathology (Figure 2I), and goblet cell hyperplasia (Figure 2J). Similar reductions in airway eosinophilia (Figures S1E and S1F) and lung pathology (Figure S1G) were noted when the microbiota was transferred via oral gavage of cecal contents to germ-free recipients. These data further support our findings that intestinal bacteria contribute to the immuno-modulatory potential of Hpb.

Helminth Infection Alters Intestinal Bacterial Communities, Resulting in Increased SCFA Production

Hpb infection has been shown to alter bacterial composition in the small intestine (Rausch et al., 2013; Reynolds et al., 2014; Walk et al., 2010), and our data indicated that transfer of bacterial communities via the feces could confer protection against allergy. To examine this in detail, we analyzed the impact of Hpb infection on bacterial community structure in the large intestine by performing sequence analysis of bacterial 16S ribosomal RNA (rRNA) genes of cecal samples taken from gnotobiotic mice colonized with a limited bacterial community, the altered Schaedler flora (ASF). As expected, the majority of bacteria in naive

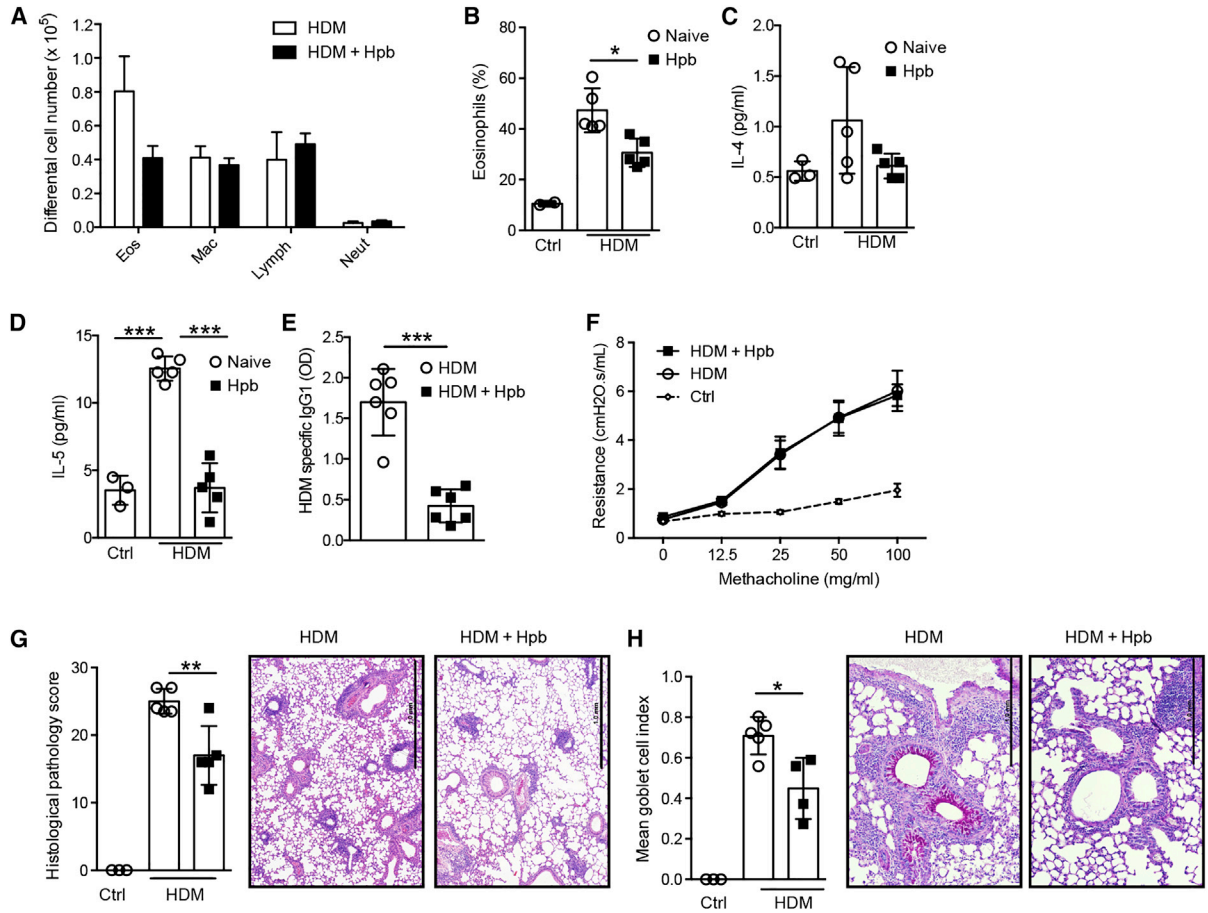

Figure 1. Infection with the Intestinal Helminth Hpb Attenuates Allergic Airway Inflammation

C57BL/6 SPF mice were infected or not with Hpb, then subjected to HDM sensitization and challenge. Mice were sacrificed 3 days after the final HDM challenge and the severity of airway inflammation was determined.

(A) Differential cell counts in the broncho-avleolar lavage fluid (BALF). Abbreviations are as follows: mac, macrophages; neut, neutrophils; eos, eosinophils; lymph, lymphocytes.

(B) Percent eosinophils within BALF cells.

(C –E) Concentrations of (C) IL-4 and (D) IL-5 cytokines within the BALF and (E) HDM-specific IgG1 in the serum. Abbreviation is as follows: OD, optical density.

(F) Measurement of AHR, as assessed by airway resistance to increasing doses of methacholine.

(G) Mean gross lung histological pathology scores with representative pictures from H&E-stained lung tissue. Scale bars represent 1 mm.

(H) Mean goblet cell index with representative periodic acid-Schiff-stained lung tissue. Scale bars represent 1 mm.

Data are expressed as the mean ± SD (n = 3 control mice and min. n = 5 mice treated with HDM extract). Each symbol represents an individual mouse. Statistical significance was determined with one-way analysis of variance (ANOVA), *p < 0.05, **p < 0.01, ***p < 0.001. Data are from one experiment and are representative of two (F) or three (A–E, G, and H) independent experiments.

ASF mice were represented by members of the Bacteroidales and Lactobacillales orders (Cahenzli et al., 2013), whereas Hpb infection led to an outgrowth of bacteria belonging to Clostridiales (Figures 3A and S2A). Growth of the HA-107 *E. coli* (Hapfelmeier et al., 2010) used to hatch Hpb larvae was also noted in the infected mice, but inoculation of naive ASF mice with 10^3 or 10^9 colony forming units (CFUs) of HA-107 *E. coli* did not prompt an outgrowth of Clostridiales (Figure S2B), indicating that this outgrowth resulted from the parasite infection itself. ASF species belonging to Clostridiales can produce SCFAs in vitro (Smith et al., 2013), prompting us to investigate SCFA concentrations in our experiments. Indeed, SCFAs were significantly increased in the cecum of Hpb-infected compared to naive ASF mice (Figure 3B). We next investigated the impact of Hpb infection on the more complex bacterial communities present in SPF mice. Principal coordinates analysis (PCoA) of operational taxonomic unit (OTU) abundances, using k-means clustering, showed an impact of Hpb infection on cecal bacterial community composition (Figures 3C and S2C). We also detected increased SCFAs in the cecum after Hpb infection of SPF mice (Figures 3D and S2D). The impact of Hpb infection on bacterial OTU abundance could also be observed using hierarchical clustering with an hclust algorithm, based on the spearman correlation co-efficient, and OTUs overrepresented in infected mice were found to be associated with increased SCFAs (Figures 3E and S2E). No consistent impact of Hpb infection on bacterial complexity was observed with the parameters of bacterial richness or the Shannon diversity index (Figures S2F–S2I).

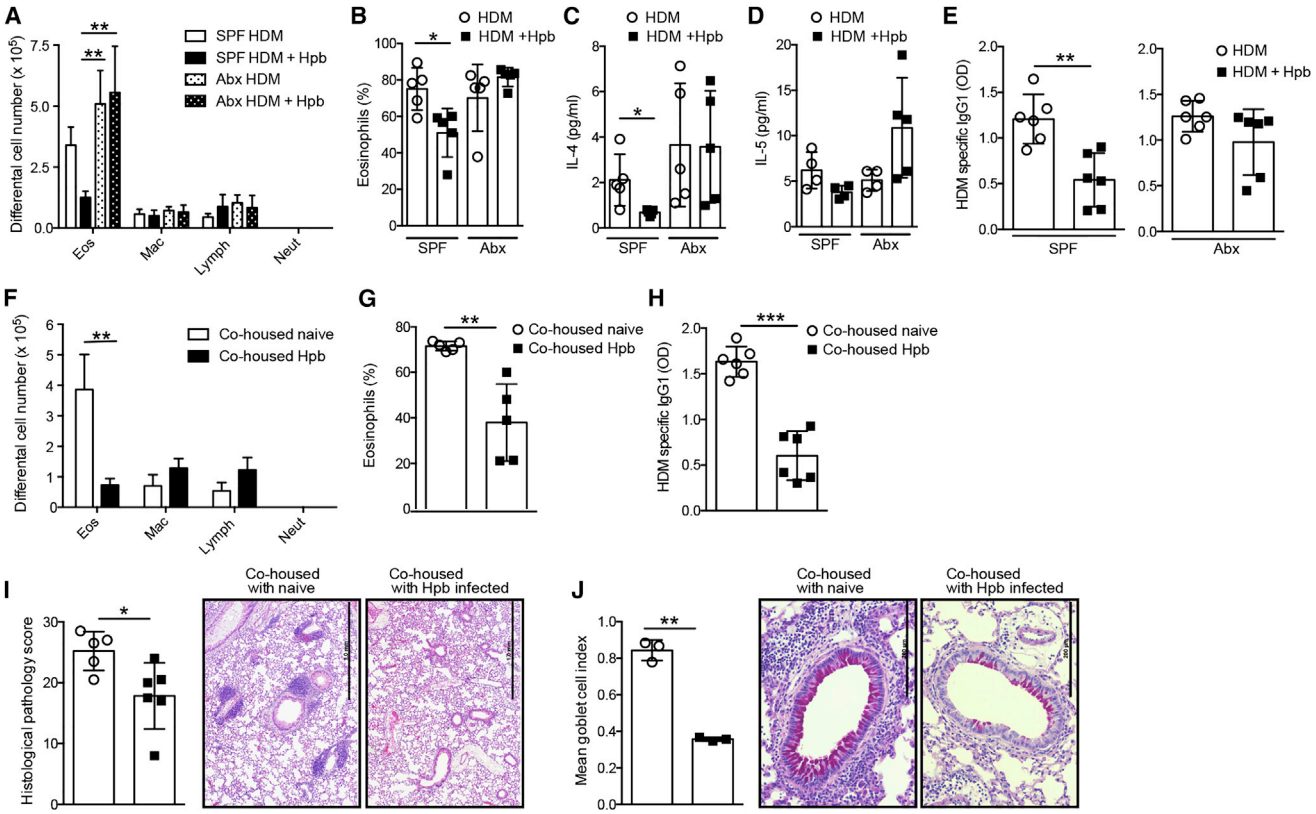

Figure 2. The Gut Microbiota Is Essential to Attenuate Allergic Airway Inflammation during Hpb Infection

(A–E) Antibiotic-treated or untreated SPF C57BL/6 mice were infected or not with Hpb, then subjected to HDM sensitization and challenge. Mice were sacrificed 3 days after the final HDM challenge and the severity of airway inflammation was determined.

(A) Differential cell counts in the BALF. Abbreviations are as follows: mac, macrophages; neut, neutrophils; eos, eosinophils; lymph, lymphocytes.

(B) Percent eosinophils within BALF cells.

(C and D) Concentrations of (C) IL-4 and (D) IL-5 cytokines within the BALF.

(E) Measurements of HDM-specific IgG1 in the serum. Abbreviation is as follows: OD, optical density.

(F–J) Antibiotic-treated recipient mice were co-housed with naive or Hpb-infected donors for 3 weeks, then subjected to HDM sensitization and challenge. Mice were sacrificed 3 days after the final HDM challenge and the severity of inflammation determined.

(F) Differential cell counts in the BALF.

(G) Percent of eosinophils of cells in the BALF.

(H) Measurement of HDM-specific IgG1 in the serum.

(I) Mean gross lung histological pathology scores with representative pictures of H&E-stained lung tissue. Scale bars represent 1 mm.

(J) Mean goblet cell index with representative pictures of periodic acid-Schiff-stained lung tissue. Scale bars represent 200 μm.

Data are expressed as the mean ± SD (n = 5 mice). Each symbol represents an individual mouse. Statistical significance was determined with two-way analysis of variance (ANOVA) (A–D, F) or Student's t test, *p < 0.05, **p < 0.01, ***p < 0.001. Data are from one experiment and are representative of three independent experiments. See also Figure S1.

Bacteria represent the major source of SCFAs in the cecum of helminth-infected mice as shown by the fact that antibiotic treatment completely abrogated SCFA production (Figure S3A). Because Hpb infection did not impact the total load of cecal bacteria (Figure S3B), the increased capacity for SCFA production in these mice probably results from changes to community structure. Thus, to determine whether the increased capacity for SCFA production could be transferred together with the altered microbial communities, we analyzed bacterial community composition and SCFA concentrations in the cecum of mice that had been co-housed with naive or helminth-infected donors, as described in Figure 2. Mice co-housed with helminth-infected donors exhibited a distinct clustering of bacterial OTUs (Figures 4A and 4B) and increased SCFAs (Figure 4C) as compared to mice co-housed with naive donors. Again, OTUs overrepresented in mice co-housed with Hpb-infected donors could be associated with increased SCFAs (Figure 4B), but only a slight impact on bacterial richness or diversity was noted (Figures S3C and S3D). The SCFAs acetate and propionate can be absorbed and enter the bloodstream, whereas butyrate is typically used locally as an energy source for intestinal epithelial cells. We therefore additionally evaluated SCFAs in the portal blood of helminth-infected mice and found significantly increased concentrations (Figure S3E).

Our data indicated that bacterial communities generate the increased SCFAs observed in helminth-infected mice. However, metazoan parasites including the intestinal helminth *Ascaris suum* have previously been reported to produce acetate (Tielens

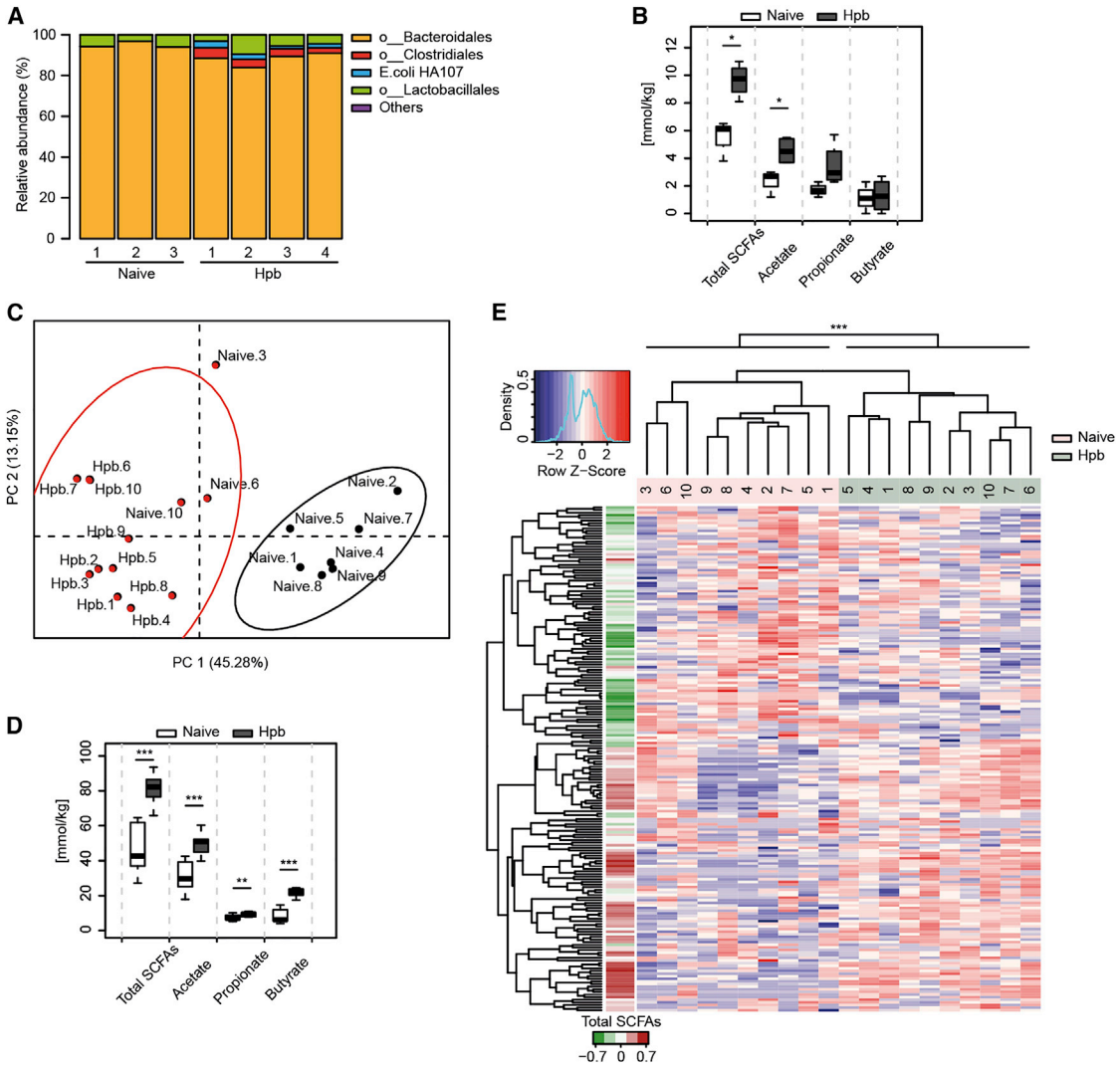

Figure 3. Hpb Infection Alters the Cecal Microbiota and Increases SCFA Concentrations

(A and B) ASF mice were infected with Hpb, cecal contents were collected, and bacterial community was analyzed by the 16S rRNA gene sequencing method.

(A) Cecal bacterial community composition at the order level. Results show OTUs relative abundances for individual mice from one experiment with n = 7 naive or Hpb-infected individuals.

(B) Cecal SCFA concentrations from the mice shown in (A). Significance was determined by unpaired Student's test.

(C–E) SPF mice were infected with Hpb, cecal contents were collected 42 days later, and the 16S rRNA genes were amplified and sequenced.

(C) Principal coordinates analysis (PCoA) using the Bray-Curtis dissimilarity based on OTU abundances. Color clustering is based on the k-means method. Results show individual mice from one experiment with n = 20 naive or Hpb-infected mice (2 cages per group).

(D) Cecal SCFA concentrations from the mice depicted in (C). Significance was determined by unpaired Student's test.

(E) OTU abundance heatmap from (C). The left color bar represents the Spearman correlation coefficient of each OTU with the total cecal SCFA concentrations. Hierarchical clustering based on the Spearman correlation coefficient was applied to order samples and OTUs.

Significance was determined by the Adonis method (*$p < 0.05$, **$p < 0.01$, ***$p < 0.001$). Data are from one experiment except for (D), where they are representative of five independent experiments. Data in (B) and (D) were generated with R boxplot with the middle bar representing the median and whiskers showing 1.5× inter-quartile range (IQR). See also Figure S2.

et al., 2010) and we confirmed that adult Hpb was able to produce small amounts of acetate when cultured in vitro in the presence of glucose (Figure S3F). However, attempts to mimic chronic Hpb infection of the small intestine by feeding ASF mice with acetate in the drinking water did not result in an outgrowth of Clostridiales in these mice (Figure S2B), indicating that helminth-derived acetate is not likely to be responsible for the changes in bacterial community structure that we observed.

Although Clostridiales were clearly associated with increased SCFA production in Hpb-infected ASF mice, it was not clear whether bacteria belonging to this order were also responsible for increased SCFAs observed in Hpb-infected SPF mice. We therefore attempted to identify bacterial OTUs that were altered by Hpb infection (as depicted in Figures 3 and S2) and in mice co-housed with helminth-infected donors (as depicted in Figure 4). To improve the taxonomic classification of OTUs assigned

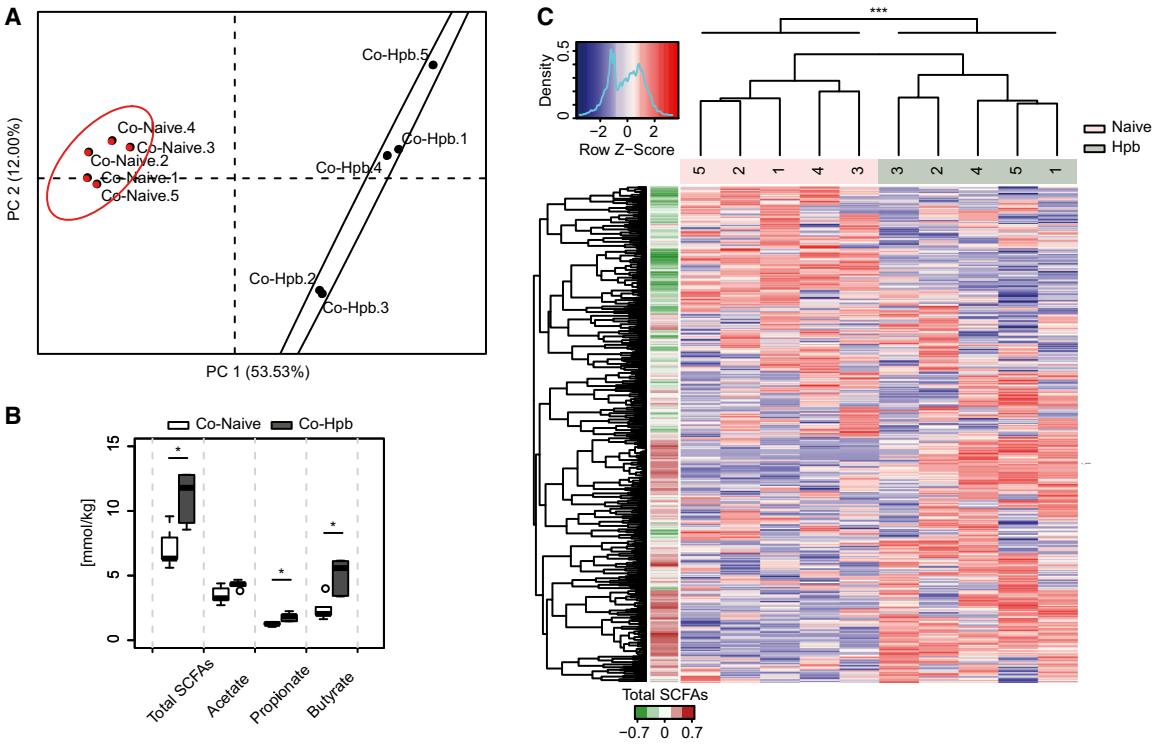

Figure 4. Hpb-Altered Microbial Communities with Increased Potential for SCFA Production Can Be Transferred to Naive Mice

Antibiotic-treated recipient mice were co-housed for 3 weeks with naive SPF or Hpb-infected mice, cecal contents were collected, and the 16S rRNA genes amplified and sequenced.

(A) Principal coordinates analysis (PCoA) using the Bray-Curtis dissimilarity based on OTU abundances. Color clustering is based on the k-means method. Results show individual mice from one experiment with n = 5 mice per group.

(B) Cecal SCFA concentrations from the mice depicted in (A). Significance was determined by unpaired Student's t test.

(C) OTU abundance heatmap from (A). The left color bar represents the Spearman correlation coefficient of each OTU with the total cecal SCFAs concentrations. Hierarchical clustering based on the Spearman correlation coefficient was applied to order samples and OTUs.

Significance was determined by the Adonis method (*$p < 0.05$, **$p < 0.01$, ***$p < 0.001$). Data are from one experiment and for (B) are representative of three independent experiments. Data in (B) were generated with R boxplot with the middle bar representing the median and whiskers showing 1.5× inter-quartile range (IQR). See also Figure S3.

to poorly characterized yet relatively abundant bacterial families (Lachnospiraceae, Ruminococcaceae, and S24-7), representative sequences for these families were used to build a phylogenetic tree and new OTU clusters within these families (defined based on the patristic distance) were then added to the original OTU taxonomy. This analysis revealed a single common OTU cluster corresponding to Clostridiales family members Lachnospiraceae. Members of this family are commonly found in the intestinal tract of mammals and are notable for containing many species capable of fermenting complex carbohydrates to SCFAs (Cotta and Forster, 2006).

Helminth Infection Alters Regulatory T Cell Function in a GPR41-Dependent Manner

It was recently reported that increasing SCFA concentrations by feeding mice a high-fiber diet attenuates HDM-induced allergic airway inflammation (Trompette et al., 2014). The same authors demonstrated that propionate treatment alters bone marrow hematopoiesis such that the lungs are seeded with immature dendritic cells that exhibit an impaired ability to promote allergic responses (Trompette et al., 2014). A second report showed that acetate treatment of mice modulates HDM-induced asthma, in this case by modulating the number and function of regulatory T (Treg) cells (Thorburn et al., 2015). In keeping with these data, we observed increased numbers of common DC precursors (CDPs) and macrophage and DC precursors (MDPs) in the bone marrow (Figures S4A and S4B) and an increase in the proportion of lung Treg cells (Figure S4C), in mice co-housed with Hpb-infected donors. We next investigated whether GPR41 (also called FFAR3) was required for the effects of Hpb infection because this receptor has been previously associated with SCFA-dependent changes to HDM-induced asthma (Trompette et al., 2014). For this purpose we infected wild-type and *Ffar3*$^{-/-}$ SPF mice with Hpb, then exposed the same mice to HDM. In line with our earlier data, helminth infection of wild-type mice led to reductions in the number (Figure 5A) and percentage (Figure 5B) of eosinophils and the amount of type 2 cell-associated cytokines (Figures 5C and 5D) in the airways. This correlated with decreased circulating HDM-specific IgG1 (Figure 5E) in helminth-infected mice. As before, helminth infection also reduced lung pathology (Figure 5F) and airway goblet cell hyperplasia (Figure 5G). In stark contrast, helminth infection of *Ffar3*$^{-/-}$

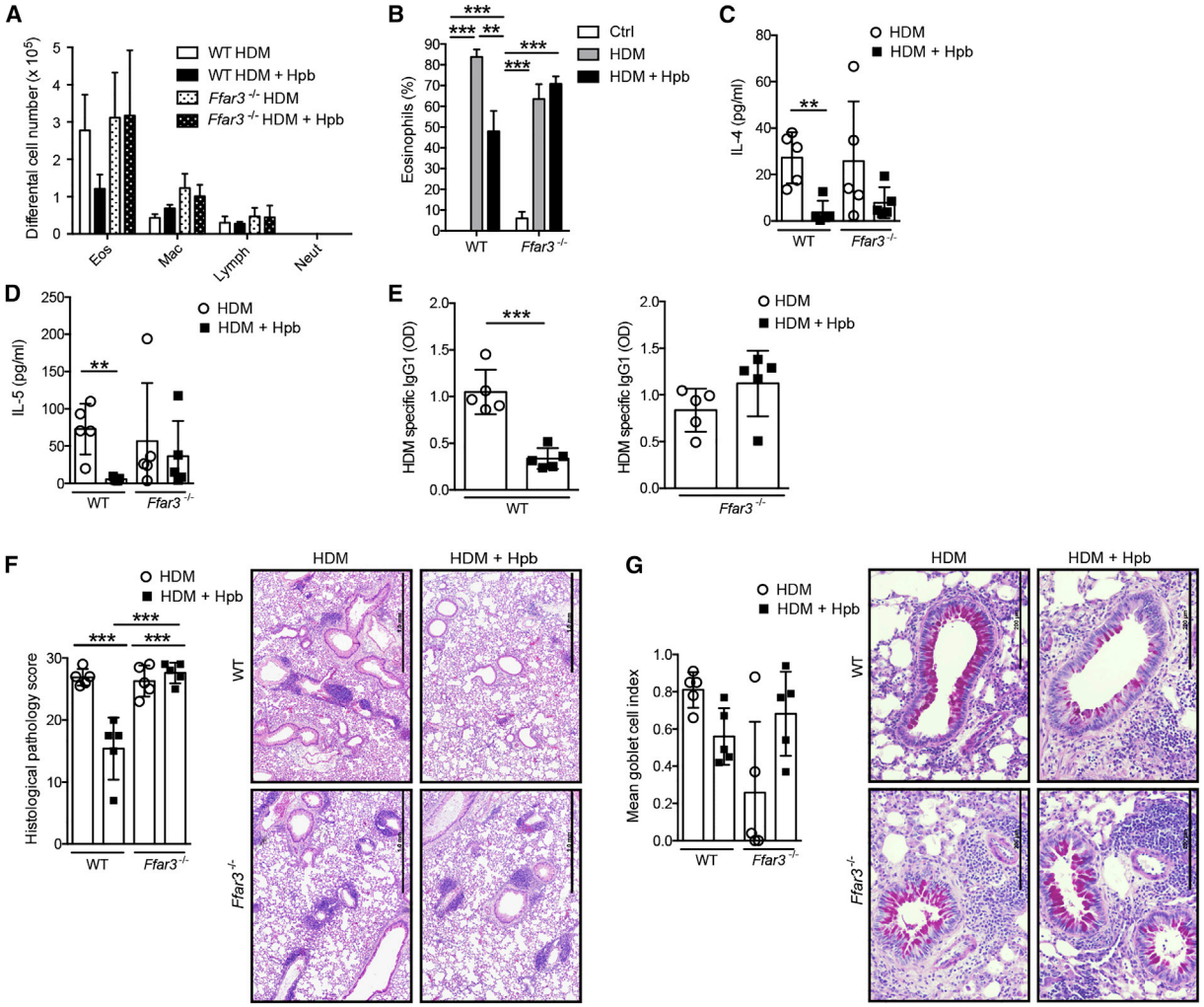

Figure 5. Hpb Infection Fails to Attenuate Allergic Airway Inflammation in *Ffar3*$^{-/-}$ Mice

C57BL/6 wild-type or *Ffar3*$^{-/-}$ SPF mice were infected or not with Hpb, then subjected to HDM sensitization and challenge. Mice were sacrificed 3 days after the final HDM challenge and the severity of airway inflammation determined.

(A) Differential cell counts in the BALF. Abbreviations are as follows: Mac, macrophages; neut, neutrophils; eos, eosinophils; lymph, lymphocytes.

(B) Percent eosinophils within BALF cells.

(C and D) Concentrations of (C) IL-4 and (D) IL-5 cytokines within the BALF.

(E) Measurement of HDM-specific IgG1 in the serum. Abbreviation is as follows: OD, optical density.

(F) Mean gross lung histological pathology scores with representative pictures of H&E-stained lung tissue. Scale bars represent 1 mm.

(G) Mean goblet cell index with representative pictures of periodic acid-Schiff-stained lung tissue. Scale bars represent 200 μm. Data are expressed mean ± SD (n = 5).

Each symbol represents an individual mouse. Statistical significance was determined with two-way analysis of variance (ANOVA) or Student's t test (E), *p < 0.05, **p < 0.01, ***p < 0.001. Data are from one experiment and are representative of three (A–E) or two (F and G) independent experiments. See also Figure S4.

mice did not improve any of the parameters measured (Figures 5A–5G). Importantly, GPR41 deficiency did not impact adult worm numbers in the small intestine (Figure S4D), and propionate or acetate supplementation failed to reduce allergic airway eosinophilia in *Ffar3*$^{-/-}$ animals (Figures S4E and S4F; Trompette et al., 2014). These data indicate that the inability of Hpb infection to modulate HDM-induced asthma in *Ffar3*$^{-/-}$ mice results from a loss of reactivity to bacterial-derived SCFAs and not from an altered response to the helminth itself.

Hpb infection has been previously reported to increase the number of interleukin-10 (IL-10)-producing Treg cells in the colon (Hang et al., 2013), a site distal to the presence of the worm, but where SCFA concentrations are increased (Figure 3D). Treg cells have also been reported to contribute to the ability of Hpb to modulate allergic airway inflammation (Wilson et al., 2005). We therefore focused our studies on the possible role of GPR41 in modulating Treg cell function in Hpb-infected mice. Hpb infection increased the concentration of IL-10 (Figure 6A) and transforming growth factor-β (TGF-β) (Figure 6B) in the lungs of HDM-challenged mice in a GPR41-dependent manner. Hpb-infected wild-type mice also exhibited a slightly increased, albeit non-significant, proportion of Treg cells in the lung (Figure 6C)

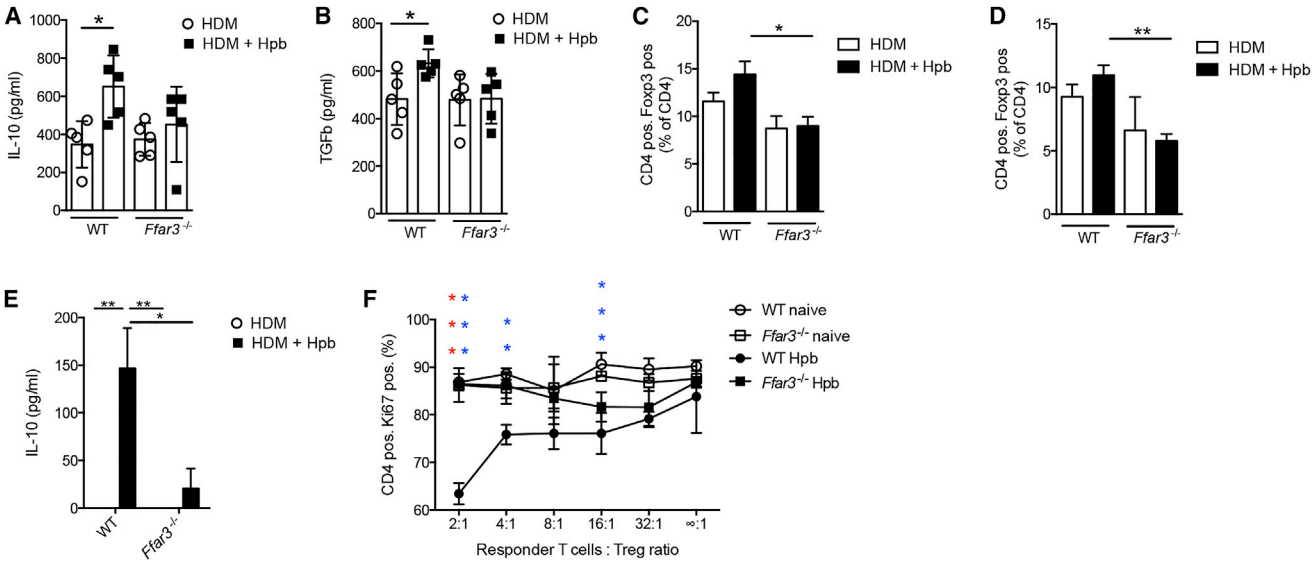

Figure 6. Hpb Infection Modulates Anti-inflammatory Cytokine Production and Treg Cell Function in the Lungs of Allergic Mice in a GPR41-Dependent Manner

SPF C57BL/6 wild-type or *Ffar3*$^{-/-}$ mice were infected or not with Hpb, then subjected to HDM sensitization and challenge. Mice were sacrificed 3 days after the final HDM challenge.

(A and B) Concentrations of (A) IL-10 and (B) TGF-β cytokines in lung tissue homogenates.

(C and D) Quantification of lung (C) and colon (D) Treg cells in WT and *Ffar3*$^{-/-}$ mice by flow cytometry analysis.

(E and F) Treg cells were isolated from the lungs of naive or Hpb-infected WT and *Ffar3*$^{-/-}$ HDM-challenged mice and cultured together with naive responder T cells in the presence of anti-CD3 and anti-CD28.

(E) Concentrations of IL-10 cytokine in the supernatant of wells containing a responder T cell:Treg cell ratio of 2:1.

(F) Proliferation as assessed by Ki67 expression. Significances in red compare WT Hpb versus *Ffar3*$^{-/-}$ Hpb and significances in blue compare WT naive versus WT Hpb-infected HDM-challenged mice.

Data are expressed as the mean ± SEM (n = 5). Statistical significance was determined with two-way analysis of variance (ANOVA); *p < 0.05, **p < 0.01, ***p < 0.001. Data in (A)–(D) are pooled from two independent experiments. Data in (E) and (F) are from one experiment and are representative of two independent experiments.

and colon (Figure 6D) and this tendency was lost in *Ffar3*$^{-/-}$ animals. To ascertain whether Treg cells exhibited an altered functional capacity after Hpb infection, we isolated Treg cells from the lung of HDM-challenged mice and cultured these together with responder CD4^{+} T cells isolated from the lymph nodes of a naive animal. Hpb infection resulted in enhanced IL-10 production (Figure 6E) and suppressor activity (Figure 6F) by Treg cells isolated from the lung of wild-type but not *Ffar3*$^{-/-}$ HDM-challenged mice. These data indicate that Hpb infection leads to the establishment of an anti-inflammatory environment in the lung, including the recruitment of IL-10-producing Treg cells, in a GPR41-dependent manner.

Increased SCFA Production Is Observed across Diverse Helminth and Host Species

To determine whether increases in SCFA availability also occur in other host-parasite settings, we examined metabolite concentrations in the colon of pigs experimentally infected with *A. suum* and in stool samples from human patients experimentally infected with *Nector americanus*. *A. suum* is a parasite of pigs that is closely related to the human parasite *A. lumbricoides*, a whipworm that infects approximately 25% of the world's population (Hotez et al., 2014), and *N. americanus*, a human hookworm, is predominantly found in the tropics and subtropics where it is estimated to infect approximately 740 million people (Hotez et al., 2014). Analysis of colon contents from pigs experimentally infected with 3 doses of 300 fertilized *A. suum* eggs on 3 consecutive days revealed increased total SCFA concentrations at 8 weeks after infection (Figure 7A). This was due to significant increases in propionate and butyrate and a trend toward increased acetate concentrations in infected pigs (Figure 7B). We next performed an analysis of SCFA concentrations in hookworm-infected patients. Stool samples were obtained from eight otherwise healthy volunteers with diet-managed (gluten-free diet for >6 months) celiac disease. All eight subjects (Pt1–Pt8) underwent voluntary infection with 20 infective larvae and were assessed 8 weeks after infection. Stool samples were collected prior to, and 8 weeks after, the second infection. From the total of eight patients, six individuals exhibited an increase in total SCFAs (Figure 7C) and two showed reduced total SCFAs after infection (Figure 7C). Changes to total SCFAs were reflected by alterations to acetate, propionate, and butyrate, but the degree to which any one metabolite was altered differed between individuals (Figure 7D). Despite a trend toward increased SCFA concentrations after hookworm infection, this did not reach statistical significance, probably reflecting the small sample size. It is important to note that diet has a major impact on SCFA concentrations and our data do not include comparison to dietary metadata. However, all patients were instructed to maintain their normal (gluten-free) diet over the course of the trial

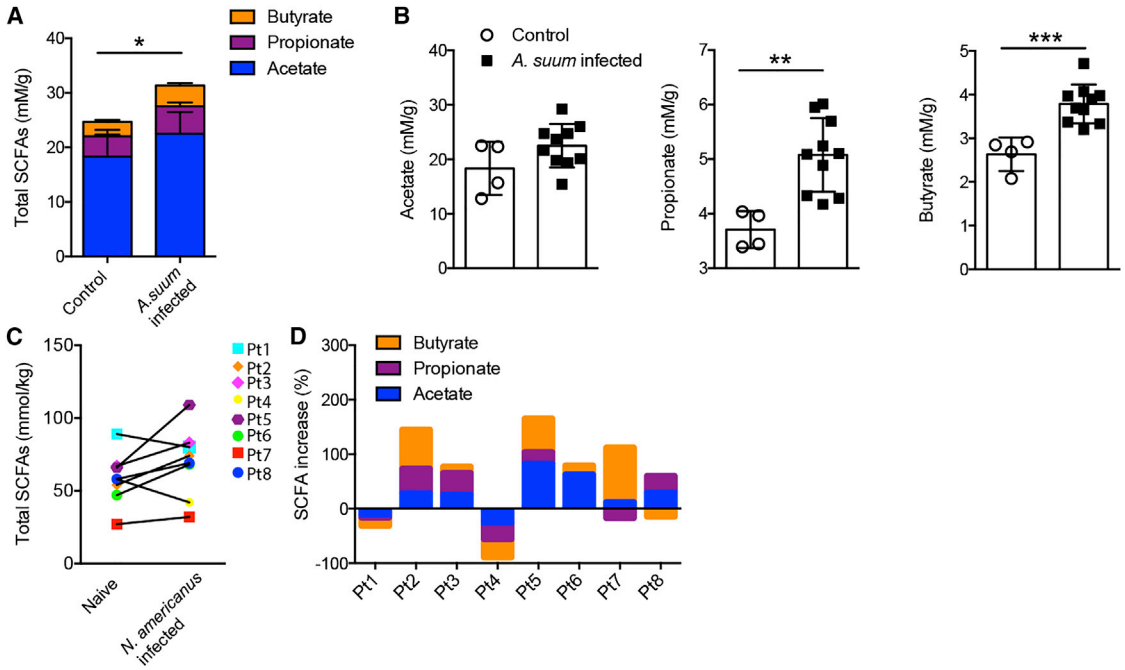

Figure 7. Helminth Infection Elevates the Concentration of SCFAs in Pigs and Humans

(A and B) GC-MS quantification of (A) total SCFA concentrations and (B) acetate, propionate, and butyrate concentrations in cecal contents taken from naive and *A. suum*-infected pigs.

(C) Total increases of SCFA concentrations of fecal samples from celiac patients before versus after hookworm (*N. americanus*) infection. Each symbol represents an individual patient (Pt).

(D) Individual percent increases of SCFA concentrations of fecal samples from celiac patients before versus after *N. americanus* infection. Data are expressed as mean ± SD.

Statistical significance was determined by Student's t test, *$p < 0.05$, **$p < 0.01$, ***$p < 0.001$.

and adherence to these instructions was regularly checked by a trained nurse. Taken together, these data raise the intriguing possibility that helminth-induced increases in bacterial-derived SCFAs might represent a phenomenon that is conserved across multiple host and parasitic species.

DISCUSSION

Previous reports have noted that helminths, or their secretions, directly regulate immune responses (Maizels et al., 2004), and hookworm infection has been consistently linked with a reduced prevalence of asthma (Leonardi-Bee et al., 2006). Here we have reported an indirect immuno-regulatory function of helminths that involves their ability to enhance bacterial-derived SCFA concentrations. As a consequence of this augmented availability of SCFAs, allergic responses are suppressed in a GPR41-dependent manner.

Declining exposure to helminths, bacterial dysbiosis, and dietary changes have all been independently proposed to underlie the rising incidence of immune and metabolic inflammatory disorders apparent in industrialized countries (Maizels, 2005; Maslowski and Mackay, 2011; Zeissig and Blumberg, 2014). SCFAs are largely derived from bacterial fermentation of complex oligosaccharides present in the diet. Our work indicates that helminth infection, intestinal bacteria, and diet might all interact to form an evolutionary conserved network that promotes immune homeostasis both through independent mechanisms and additionally through unifying mediators, such as SCFAs. In this regard, it is interesting that people living in poor regions of the developing world rarely suffer from allergies (Wjst and Boakye, 2007), are exposed to intestinal helminths (Hotez et al., 2014), typically consume diets richer in fermentable fibers, and exhibit higher stool concentrations of SCFAs (De Filippo et al., 2010) than those living in industrialized countries.

Infection with intestinal helminths probably increases bacterial-derived SCFAs through multiple mechanisms and might involve direct interactions between helminths and bacteria or indirect interactions whereby helminth-induced immune responses result in changes to the mucosal environment. Such immune-driven changes might also underlie the remarkable convergence in the ability of diverse helminth species to increase intestinal SCFAs. Such convergence also indicates a strong evolutionary benefit for the parasite to modulate metabolite levels. One potential benefit could include the known ability of SCFAs to promote host regulatory T cell responses (Arpaia et al., 2013; Furusawa et al., 2013; Smith et al., 2013) that could act to limit immuno-pathology and promote parasite chronicity. In keeping with this hypothesis, we observed that Hpb infection led to an increased production of anti-inflammatory cytokines and potentiated Treg cell suppressor activity in the lung, likely contributing to the helminth-induced modulation of allergic asthma. Our finding that these responses required GPR41 indicates that increased SCFA availability contributes, at least in part, to enhanced Treg cell suppressor function after helminth

infection. Of note, the same patients for whom we analyzed SCFAs exhibited increased frequencies of intestinal $CD4^+$ $Foxp3^+$ T cells after hookworm infection (Croese et al., 2015). Environmental or experimental helminth infection has also been reported to reduce the severity of other inflammatory diseases including arthritis (Salinas-Carmona et al., 2009), inflammatory bowel disease (Weinstock, 2006), and multiple sclerosis (Correale and Farez, 2011). Thus, future studies investigating the impact of helminth infection on SCFAs in individuals living in helminth-endemic regions or in clinically infected patients would be of great interest.

Although our study highlights an indirect mechanism by which helminths modulate host immunity, it is likely that helminths also impact immune cell function in a direct manner. Indeed, there is a wealth of evidence detailing the ability of these organisms to secrete immuno-modulatory products (Maizels et al., 2004). Hpb-secreted products also possess the ability to modulate DC function (Massacand et al., 2009) and can promote immunological tolerance to allograft transplants (Johnston et al., 2015). Although our current work indicates that bacterial SCFAs contribute to the ability of Hpb to modulate Treg cell function, previous reports, including work from our own laboratory, demonstrate that this helminth can also modulate Treg cell function directly (Grainger et al., 2010; Mosconi et al., 2015). Helminth products documented to directly modulate airway inflammation include Hpb excretory-secretory products (McSorley et al., 2012) and *Acanthocheilonema viteae* recombinant Av17 cystatin (Schnoeller et al., 2008). However, numerous obstacles complicate the use of live parasites or potentially immunogenic parasitic products in the treatment of inflammatory disorders. Our data indicate that improved therapeutic approaches might also result from the analysis of helminth-bacterial interactions in the gut.

In summary, we demonstrate how intestinal helminth infection changes the intestinal microbiota and increases SCFA production. As a consequence, allergic airway inflammation is attenuated in the host in a GPR41-dependent manner. This work provides an example of how parasites drive a functional cross talk with the intestinal microbiota and how this cross talk affects immune mechanisms of the host. Mutual adaptation of intestinal parasites and the intestinal microbiota is likely to also have consequences for other inflammatory diseases or for host physiology outside the immune system.

EXPERIMENTAL PROCEDURES

Ethics Statement

All animal experiments were approved by the Service de la consommation et des affaires vétérinaires (1066 Épalinges, Canton of Vaud, Switzerland) with the authorization numbers 2238 and 2540.

Mice, Parasites, and Treatments

C57BL/6 and *Ffar3*$^{-/-}$ mice were bred and maintained under specific-pathogen-free (SPF) conditions at École Polytechnique Fédérale de Lausanne (EPFL), Switzerland. All mice were fed with standard breeding diet 3242 (KLIBA NAFAG) including 3.5% crude fibers. To standardize the intestinal bacteria within different groups of SPF mice analyzed within one experiment, all mice were co-housed, or beddings were mixed, for 3 weeks prior to parasite infection. Where indicated, mice were then pre-infected orally with 200 L3 Hpb. After Hpb infection, co-housing or bedding mixes were stopped for the rest of the experiment. Adult worm burdens were determined by manual counting of the small intestinal contents under a dissecting microscope.

HDM-Induced Allergic Airway Inflammation

Mice were anesthetized with isoflurane and challenged intranasally with 15 μl of HDM (Greer Laboratories) in 30 μl sterile saline every other day three times per week for 3 consecutive weeks with a total of nine exposures. For all experiments, HDM challenges started 2 weeks after Hpb infection. Airway inflammation and BALF infiltrates were examined 3 days after the last HDM challenge. Total cell numbers were determined with a Guava PCA Cell Counter (Millipore). Differential cell counts were performed on cytospins stained with Diff-Quik solution (Siemens Healthcare Diagnostics) and 200 cells per sample counted. Lung function and airway hyper-responsiveness were quantified via the forced oscillation system (Flexivent, Scireq) as previously described (Gollwitzer et al., 2014).

Antibiotic Treatment and Co-housing

Mice were treated with 2.5 mg/ml enrofloxacin in drinking water for 2 weeks, followed by 0.8 mg/ml of amoxicillin and 0.114 mg/ml clavulanic acid in drinking water for a minimum of 2 further weeks prior to infection. Treatment with amoxicillin and clavulanic acid was then continued throughout the remainder of the experiment. For co-housing experiments, antibiotic treatment was discontinued and mice co-housed with naive or day 21 Hpb-infected SPF mice for a period of 3 weeks prior to HDM exposure. The effectiveness of antibiotic treatment was routinely assessed by plating of cecal contents under standard aerobic and anaerobic conditions and by microscopic analysis of fecal smears stained with Sytox Green nucleic acid stain (Life Technologies) and Gram staining (Sigma-Aldrich). Fecal smears were additionally checked for the presence of fungi by calcofluor white staining (Sigma-Aldrich).

Generation of Bacteriologically Sterile Hpb Larvae and Ex Vivo Worm Cultures

Bacteriologically sterile Hpb infection of antibiotic-treated mice was achieved using infective larvae (L3) hatched from fecal cultures and subjected to successive washings with PBS and RPMI containing enrofloxacin (5 mg/ml), amoxicillin (2 mg/ml), and clavulanic acid (0.2 mg/ml). Alternatively, adult worms were collected from intestinal contents of infected mice, washed in PBS and RPMI containing 0.2 mg/ml gentamycin, 200 IU/ml penicillin, and 200 μg/ml streptomycin (GIBCO), and cultured overnight at 37°C in RPMI 1640 (GIBCO) containing 0.1 mg/ml gentamycin, 100 IU/ml penicillin, 100 μg/ml streptomycin, and 1% glucose (Sigma-Aldrich). Excreted eggs were collected from the medium and hatched by incubation on nematode growth media plates covered with auxotrophic *E. coli* HA107 (Hapfelmeier et al., 2010) for a period of 4–5 days at 27°C. The sterility of infective larvae was determined by standard microbial plating on bacterial and fungal growth media. For the culture of adult worms, L5 Hpb were collected from the intestine of infected mice and washed extensively as described for L3 above. 50 L5 Hpb were cultured in 100 μl L5 culture media and the supernatant was collected after 48 hr.

Measurements of Cytokines, Antibodies, and SCFAs

IL-4 and IL-5 cytokines were analyzed with mouse Milliplex kits (Merk Millipore) according to the manufacturer's instructions and read on a Luminex 100/200 analyzer. ELISA assays for HDM-specific IgG1 were performed as previously described (Trompette et al., 2014). IL-10 and TGF-β were analyzed with ELISA kits according to the manufacturer's instructions (eBioscience). SCFAs were analyzed by the Mass Spectrometry Service of the Institute of Chemical Sciences and Engineering (EPFL, Switzerland) or by Metabolomics Australia (Bayliss Building, University of Western Australia). Details are provided in Supplemental Experimental Procedures.

Histology

Formalin-fixed lung sections were embedded in paraffin, sectioned at 4 μm, and stained with hematoxylin and eosin or periodic acid-Schiff via standard protocols. Histopathological scores were performed in a blind fashion by a European board-certified veterinary pathologist with a light microscope Nikon Eclipse E400. The histopathological scoring is detailed in Supplemental Experimental Procedures.

16S rRNA Gene Sequencing

Bacterial community analysis was performed with the 16S rRNA gene sequencing method. In brief, DNA was extracted from cecal contents and the V1-V2 region of the bacterial 16S rRNA gene was amplified by PCR. Amplicons were purified and sequenced on an Illumina MiSeq platform. Sequences were analyzed with the QIIME software package. See Supplemental Experimental Procedures for full details.

In Vitro Treg Cell Suppression Assay

Lungs were digested with collagenase IV (Worthington biochemical corporation) in Iscove's modified Dulbecco's medium for 45 min at 37°C and filtered through 40 μm gauze (BD Biosciences) to generate single-cell suspensions that were then subjected to MACS sorting to enrich Treg cells ($CD4^+CD25^+$) according to the manufacturer instructions (Miltenyi Biotec). $CD4^+CD25^-$ responder T cells were MACS sorted from the lymph nodes of naive mice. Lung Treg cells and responder T cells were co-cultured at different ratios (responder T cells 2.5×10^4 cells/well and Treg cells at 1.25×10^4 at a 2:1 ratio) in U-bottom 96-well plates in the presence of soluble 0.75 μg/ml α-CD3 (clone 37.51) and 4 μg/ml α-CD28 (clone 145-2C11) for 3 days (eBioscience) (Collison and Vignali, 2011). Cells were stained, fixed, and permeabilized for flow cytometry with the Foxp3 staining buffer kit (eBiosciences) with the following antibodies CD4 APC/Cy (clone RM4-5, Biolegend), CD25 PE/Cy7 (PC61, Biolegend), Foxp3 AF647 (MF23, BD Biosciences), and Ki67 PercpCy5.5 (clone B56, BD Biosciences) using the LSRII (BD Biosciences). Data were acquired on an LSRII flow cytometer (BD Biosciences) and analyzed with FlowJo software (Tree Star).

Treg Cell Flow Cytometry

Lungs were digested as above. Colons were incubated with PBS containing EDTA at 37°C for 15 min then digested twice for 35 min with a cocktail of collagenase D (1 mg/ml, Roche), dispase I (0.1 mg/ml, Roche), and DNase I (333 μg/ml, Sigma), smashed and filtered through a 40 μm gauze (BD Biosciences). Single-cell suspensions were then stained for flow cytometry with the following antibodies: CD4 Pacific blue (clone GK1.5), CD103 biotin (clone M290 or 2E7), CD25 PE-cy7 (clone PC61), PD1 PE (clone RMP1-30), GITR FITC (clone DTA-1), and streptavidin APC were purchased from BD Biosciences or Biolegend. FoxP3 AlexaFluor (clone FJK-16a, eBioscience) and Ki-67 PE (clone B56, BD Biosciences) were used in combination with a FoxP3 staining kit (eBioscience).

Porcine Roundworm Infection

The animal experiment was conducted in accordance with the European Animal Welfare Directives and VICH Guidelines for Good Clinical Practice, and ethical approval to conduct the studies was obtained from the Ethical Committee of the Faculty of Veterinary Medicine, Ghent University (EC2013/109), who has also approved the document. 24 female and male Rattlerow Seghers hybrid pigs (10 weeks old) were included in the study. The animals had free access to feed and water. 20 of these pigs were infected with *A. suum* fertilized eggs, and the remaining 4 pigs were included in the trial as non-infected naive control animals. *A. suum* eggs were obtained from adult gravid female *A. suum* worms, collected at the local abattoir and incubated in 0.1% (w/v) KCr_2O_2 until embryonation. The 20 pigs in the infected group received three doses of 300 fertilized eggs on 3 consecutive days via oral intubation. Eggs per gram feces were monitored every 2 days from day 47 post-infection onward. At day 54 post-infection, all pigs were euthanized. Intestinal contents of all of the 24 pigs were sampled at the colon, 30 cm distal from the junction of the caecum and proximal colon. The samples were snap-frozen in liquid nitrogen and preserved at −80°C until further processing for SCFA determination. The numbers of adult worms present in the small intestine were counted manually. Out of the 20 infected animals, 10 were finally selected for the SCFA analysis, based on their high worm burden.

Human Participants and *N. americanus* Infections

Eight otherwise healthy volunteers with diet-managed (gluten-free diet for >6 months) HLA-DQ2+ or HLA-DQ8+ celiac disease were included in the study (mean age 52 years, range 39–67, 3 male, 5 female). All subjects had been pre-infected with *N. americanus* between 2008 and 2010 as part of a previous clinical trial (Daveson et al., 2011) and underwent anthelminthic therapy (200 mg mebendazole twice daily for 3 days) 6 weeks prior to the commencement of the present study which involved infection with a total of 20 larvae (10 L3 at week 0 and 10 L3 at week 4). The current study, designated HREC/07/QPAH/115, was approved in 2012 by the Human Research Ethics Committee (EC00167) at the Centres for Health Research, Princess Alexandra Hospital. The trials were registered at ClinicalTrials.gov, with the identifiers NCT: NCT00671138 (2008) and NCT: NCT01661933 (2012). Written informed consent was obtained from all subjects enrolled in the study. *N. americanus* ova were collected from two volunteers initially pre-infected with infective third-stage larvae (L3) from a line donated by Professor David Pritchard (University of Nottingham) and maintained in-house through re-inoculation.

Statistical Analysis

Statistical analyses were performed with a Student's t test, one-way or two-way ANOVA followed by Tukey's multiple comparison post test. For all experiments, p values are indicated as $*p < 0.05$, $**p < 0.01$, or $***p < 0.001$. Graph generation and statistical analyses were performed with Prism v.6c software (GraphPad).

ACCESSION NUMBERS

Sequence data are available at the European Nucleotide Archive (ENA): PRJEB10642.

SUPPLEMENTAL INFORMATION

Supplemental Information includes four figures, two tables, and Supplemental Experimental Procedures and can be found with this article online at http://dx.doi.org/10.1016/j.immuni.2015.09.012.

AUTHOR CONTRIBUTIONS

M.M.Z., B.J.M., and N.L.H. conceived of and designed the study. M.M.Z, L.L., L.K.D., I.M., K.S., and K.D.M. performed experiments. M.M.Z., A.R., and A.P. analyzed the data. A.R. generated a subset of the 16S rRNA gene sequences and performed all of the microbiota analysis, and A.W.W. generated a subset of the 16S rRNA gene sequences. J.R. provided support for microbiota analysis. A.P. performed histopathological scoring. L.M. performed SCFA analysis. O.P. and P.G. provided *A. suum*-infected porcine fecal samples. A.L., J.C., and P.R.G. provided *N. americanus*-infected human fecal samples. A.J.M. generated and provided HA107 *E. coli* and T.J. provided *Ffar3*$^{-/-}$ mice. M.M.Z., A.R., T.J., B.J.M., A.W.W., P.R.G., A.L., and N.L.H. provided critical analysis and discussions. M.M.Z. and N.L.H. wrote the paper.

ACKNOWLEDGMENTS

We thank Manuel Kulagin for technical help, Pierre Bonnaventure for portal vein blood sampling, Francisco Sepulveda for technical assistance in GS-MS acquisition, and Dorothee Hahne (Metabolomics Australia, University of Western Australia) for human samples SCFA isolation, acquisition, and analysis. We also thank Cristina Cartoni (Phenotyping Unit, EPFL) for Milliplex analysis, Jessica Dessimoz and her team from the Histology Core Facility (EPFL), Miguel Garcia and his team from the Flow Cytometry Core Facility (EPFL), and staff from the EPFL CPG animal house for excellent animal care. The computations were partially performed at the Vital-IT Center for high-performance computing of the SIB Swiss Institute of Bioinformatics (http://www.vital-it.ch). The research leading to these results has received funding from the European Research Council under the European Union's Seventh Framework Programme (FP/2007-2013) / ERC Grant Agreement n. 310948. Funding for A.W.W. and a subset of the 16S rRNA gene sequencing was provided by the Wellcome Trust (grant number WT 098051). The funders had no role in study design, data collection and analysis, decision to publish, or preparation of the manuscript.

Received: December 30, 2014
Revised: July 12, 2015
Accepted: September 28, 2015
Published: October 27, 2015

REFERENCES

Arpaia, N., Campbell, C., Fan, X., Dikiy, S., van der Veeken, J., deRoos, P., Liu, H., Cross, J.R., Pfeffer, K., Coffer, P.J., and Rudensky, A.Y. (2013). Metabolites produced by commensal bacteria promote peripheral regulatory T-cell generation. Nature *504*, 451–455.

Broadhurst, M.J., Ardeshir, A., Kanwar, B., Mirpuri, J., Gundra, U.M., Leung, J.M., Wiens, K.E., Vujkovic-Cvijin, I., Kim, C.C., Yarovinsky, F., et al. (2012). Therapeutic helminth infection of macaques with idiopathic chronic diarrhea alters the inflammatory signature and mucosal microbiota of the colon. PLoS Pathog. *8*, e1003000.

Cahenzli, J., Köller, Y., Wyss, M., Geuking, M.B., and McCoy, K.D. (2013). Intestinal microbial diversity during early-life colonization shapes long-term IgE levels. Cell Host Microbe *14*, 559–570.

Collison, L.W., and Vignali, D.A. (2011). In vitro Treg suppression assays. Methods Mol. Biol. *707*, 21–37.

Cooper, P.J., Chico, M.E., Rodrigues, L.C., Ordonez, M., Strachan, D., Griffin, G.E., and Nutman, T.B. (2003). Reduced risk of atopy among school-age children infected with geohelminth parasites in a rural area of the tropics. J. Allergy Clin. Immunol. *111*, 995–1000.

Correale, J., and Farez, M.F. (2011). The impact of environmental infections (parasites) on MS activity. Mult. Scler. *17*, 1162–1169.

Cotta, M., and Forster, R. (2006). The family Lachnospiraceae, including the genera Butyrivibrio, Lachnospira and Rosburia. Prokaryotes *4*, 1002–1021.

Croese, J., Giacomin, P., Navarro, S., Clouston, A., McCann, L., Dougall, A., Ferreira, I., Susianto, A., O'Rourke, P., Howlett, M., et al. (2015). Experimental hookworm infection and gluten microchallenge promote tolerance in celiac disease. J. Allergy Clin. Immunol. *135*, 508–516.

Daveson, A.J., Jones, D.M., Gaze, S., McSorley, H., Clouston, A., Pascoe, A., Cooke, S., Speare, R., Macdonald, G.A., Anderson, R., et al. (2011). Effect of hookworm infection on wheat challenge in celiac disease–a randomised double-blinded placebo controlled trial. PLoS ONE *6*, e17366.

De Filippo, C., Cavalieri, D., Di Paola, M., Ramazzotti, M., Poullet, J.B., Massart, S., Collini, S., Pieraccini, G., and Lionetti, P. (2010). Impact of diet in shaping gut microbiota revealed by a comparative study in children from Europe and rural Africa. Proc. Natl. Acad. Sci. USA *107*, 14691–14696.

Dorrestein, P.C., Mazmanian, S.K., and Knight, R. (2014). Finding the missing links among metabolites, microbes, and the host. Immunity *40*, 824–832.

Furusawa, Y., Obata, Y., Fukuda, S., Endo, T.A., Nakato, G., Takahashi, D., Nakanishi, Y., Uetake, C., Kato, K., Kato, T., et al. (2013). Commensal microbe-derived butyrate induces the differentiation of colonic regulatory T cells. Nature *504*, 446–450.

Garrett, W.S., Lord, G.M., Punit, S., Lugo-Villarino, G., Mazmanian, S.K., Ito, S., Glickman, J.N., and Glimcher, L.H. (2007). Communicable ulcerative colitis induced by T-bet deficiency in the innate immune system. Cell *131*, 33–45.

Gause, W.C., Wynn, T.A., and Allen, J.E. (2013). Type 2 immunity and wound healing: evolutionary refinement of adaptive immunity by helminths. Nat. Rev. Immunol. *13*, 607–614.

Gollwitzer, E.S., Saglani, S., Trompette, A., Yadava, K., Sherburn, R., McCoy, K.D., Nicod, L.P., Lloyd, C.M., and Marsland, B.J. (2014). Lung microbiota promotes tolerance to allergens in neonates via PD-L1. Nat. Med. *20*, 642–647.

Grainger, J.R., Smith, K.A., Hewitson, J.P., McSorley, H.J., Harcus, Y., Filbey, K.J., Finney, C.A., Greenwood, E.J., Knox, D.P., Wilson, M.S., et al. (2010). Helminth secretions induce de novo T cell Foxp3 expression and regulatory function through the TGF-β pathway. J. Exp. Med. *207*, 2331–2341.

Hang, L., Blum, A.M., Setiawan, T., Urban, J.P., Jr., Stoyanoff, K.M., and Weinstock, J.V. (2013). Heligmosomoides polygyrus bakeri infection activates colonic Foxp3+ T cells enhancing their capacity to prevent colitis. J. Immunol. *191*, 1927–1934.

Hapfelmeier, S., Lawson, M.A., Slack, E., Kirundi, J.K., Stoel, M., Heikenwalder, M., Cahenzli, J., Velykoredko, Y., Balmer, M.L., Endt, K., et al. (2010). Reversible microbial colonization of germ-free mice reveals the dynamics of IgA immune responses. Science *328*, 1705–1709.

Herbst, T., Sichelstiel, A., Schär, C., Yadava, K., Bürki, K., Cahenzli, J., McCoy, K., Marsland, B.J., and Harris, N.L. (2011). Dysregulation of allergic airway inflammation in the absence of microbial colonization. Am. J. Respir. Crit. Care Med. *184*, 198–205.

Hotez, P.J., Alvarado, M., Basáñez, M.G., Bolliger, I., Bourne, R., Boussinesq, M., Brooker, S.J., Brown, A.S., Buckle, G., Budke, C.M., et al. (2014). The global burden of disease study 2010: interpretation and implications for the neglected tropical diseases. PLoS Negl. Trop. Dis. *8*, e2865.

Johnston, C., McSorley, H., Smyth, D., Anderton, S., Wigmore, S., and Maizels, R. (2015). A role for helminth parasites in achieving immunological tolerance in transplantation. Lancet *385* (*Suppl 1*), S50.

Khan, A.R., and Fallon, P.G. (2013). Helminth therapies: translating the unknown unknowns to known knowns. Int. J. Parasitol. *43*, 293–299.

Leonardi-Bee, J., Pritchard, D., and Britton, J. (2006). Asthma and current intestinal parasite infection: systematic review and meta-analysis. Am. J. Respir. Crit. Care Med. *174*, 514–523.

Macpherson, A.J., and Harris, N.L. (2004). Interactions between commensal intestinal bacteria and the immune system. Nat. Rev. Immunol. *4*, 478–485.

Maizels, R.M. (2005). Infections and allergy - helminths, hygiene and host immune regulation. Curr. Opin. Immunol. *17*, 656–661.

Maizels, R.M., Balic, A., Gomez-Escobar, N., Nair, M., Taylor, M.D., and Allen, J.E. (2004). Helminth parasites–masters of regulation. Immunol. Rev. *201*, 89–116.

Maizels, R.M., and Yazdanbakhsh, M. (2003). Immune regulation by helminth parasites: cellular and molecular mechanisms. Nat. Rev. Immunol. *3*, 733–744.

Maslowski, K.M., and Mackay, C.R. (2011). Diet, gut microbiota and immune responses. Nat. Immunol. *12*, 5–9.

Massacand, J.C., Stettler, R.C., Meier, R., Humphreys, N.E., Grencis, R.K., Marsland, B.J., and Harris, N.L. (2009). Helminth products bypass the need for TSLP in Th2 immune responses by directly modulating dendritic cell function. Proc. Natl. Acad. Sci. USA *106*, 13968–13973.

McSorley, H.J., O'Gorman, M.T., Blair, N., Sutherland, T.E., Filbey, K.J., and Maizels, R.M. (2012). Suppression of type 2 immunity and allergic airway inflammation by secreted products of the helminth *Heligmosomoides polygyrus*. Eur. J. Immunol. *42*, 2667–2682.

Mishra, P.K., Patel, N., Wu, W., Bleich, D., and Gause, W.C. (2013). Prevention of type 1 diabetes through infection with an intestinal nematode parasite requires IL-10 in the absence of a Th2-type response. Mucosal Immunol. *6*, 297–308.

Mosconi, I., Dubey, L.K., Volpe, B., Esser-von Bieren, J., Zaiss, M.M., Lebon, L., Massacand, J.C., and Harris, N.L. (2015). Parasite proximity drives the expansion of regulatory T cells in Peyer's patches following intestinal helminth infection. Infect. Immun. *83*, 3657–3665.

Osada, Y., Yamada, S., Nabeshima, A., Yamagishi, Y., Ishiwata, K., Nakae, S., Sudo, K., and Kanazawa, T. (2013). *Heligmosomoides polygyrus* infection reduces severity of type 1 diabetes induced by multiple low-dose streptozotocin in mice via STAT6- and IL-10-independent mechanisms. Exp. Parasitol. *135*, 388–396.

Osborne, L.C., Monticelli, L.A., Nice, T.J., Sutherland, T.E., Siracusa, M.C., Hepworth, M.R., Tomov, V.T., Kobuley, D., Tran, S.V., Bittinger, K., et al. (2014). Coinfection. Virus-helminth coinfection reveals a microbiota-independent mechanism of immunomodulation. Science *345*, 578–582.

Rausch, S., Held, J., Fischer, A., Heimesaat, M.M., Kühl, A.A., Bereswill, S., and Hartmann, S. (2013). Small intestinal nematode infection of mice is associated with increased enterobacterial loads alongside the intestinal tract. PLoS ONE *8*, e74026.

Reynolds, L.A., Smith, K.A., Filbey, K.J., Harcus, Y., Hewitson, J.P., Redpath, S.A., Valdez, Y., Yebra, M.J., Finlay, B.B., and Maizels, R.M. (2014). Commensal-pathogen interactions in the intestinal tract: lactobacilli promote infection with, and are promoted by, helminth parasites. Gut Microbes *5*, 522–532.

Salinas-Carmona, M.C., de la Cruz-Galicia, G., Pérez-Rivera, I., Solís-Soto, J.M., Segoviano-Ramirez, J.C., Vázquez, A.V., and Garza, M.A. (2009). Spontaneous arthritis in MRL/lpr mice is aggravated by *Staphylococcus aureus*

and ameliorated by *Nippostrongylus brasiliensis* infections. Autoimmunity *42*, 25–32.

Schnoeller, C., Rausch, S., Pillai, S., Avagyan, A., Wittig, B.M., Loddenkemper, C., Hamann, A., Hamelmann, E., Lucius, R., and Hartmann, S. (2008). A helminth immunomodulator reduces allergic and inflammatory responses by induction of IL-10-producing macrophages. J. Immunol. *180*, 4265–4272.

Smith, P.M., Howitt, M.R., Panikov, N., Michaud, M., Gallini, C.A., Bohlooly-Y, M., Glickman, J.N., and Garrett, W.S. (2013). The microbial metabolites, short-chain fatty acids, regulate colonic Treg cell homeostasis. Science *341*, 569–573.

Thorburn, A.N., McKenzie, C.I., Shen, S., Stanley, D., Macia, L., Mason, L.J., Roberts, L.K., Wong, C.H., Shim, R., Robert, R., et al. (2015). Evidence that asthma is a developmental origin disease influenced by maternal diet and bacterial metabolites. Nat. Commun. *6*, 7320.

Tielens, A.G., van Grinsven, K.W., Henze, K., van Hellemond, J.J., and Martin, W. (2010). Acetate formation in the energy metabolism of parasitic helminths and protists. Int. J. Parasitol. *40*, 387–397.

Trompette, A., Gollwitzer, E.S., Yadava, K., Sichelstiel, A.K., Sprenger, N., Ngom-Bru, C., Blanchard, C., Junt, T., Nicod, L.P., Harris, N.L., and Marsland, B.J. (2014). Gut microbiota metabolism of dietary fiber influences allergic airway disease and hematopoiesis. Nat. Med. *20*, 159–166.

Turnbaugh, P.J., Bäckhed, F., Fulton, L., and Gordon, J.I. (2008). Diet-induced obesity is linked to marked but reversible alterations in the mouse distal gut microbiome. Cell Host Microbe *3*, 213–223.

Walk, S.T., Blum, A.M., Ewing, S.A., Weinstock, J.V., and Young, V.B. (2010). Alteration of the murine gut microbiota during infection with the parasitic helminth *Heligmosomoides polygyrus*. Inflamm. Bowel Dis. *16*, 1841–1849.

Weinstock, J.V. (2006). Helminths and mucosal immune modulation. Ann. N Y Acad. Sci. *1072*, 356–364.

Wilson, M.S., Taylor, M.D., Balic, A., Finney, C.A., Lamb, J.R., and Maizels, R.M. (2005). Suppression of allergic airway inflammation by helminth-induced regulatory T cells. J. Exp. Med. *202*, 1199–1212.

Wjst, M., and Boakye, D. (2007). Asthma in Africa. PLoS Med. *4*, e72.

Wu, S., Li, R.W., Li, W., Beshah, E., Dawson, H.D., and Urban, J.F., Jr. (2012). Worm burden-dependent disruption of the porcine colon microbiota by *Trichuris suis* infection. PLoS ONE *7*, e35470.

Zeissig, S., and Blumberg, R.S. (2014). Life at the beginning: perturbation of the microbiota by antibiotics in early life and its role in health and disease. Nat. Immunol. *15*, 307–310.

Immunity

Supplemental Information

The Intestinal Microbiota Contributes to the Ability of Helminths to Modulate Allergic Inflammation

Mario M. Zaiss, Alexis Rapin, Luc Lebon, Lalit Kumar Dubey, Ilaria Mosconi, Kerstin Sarter, Alessandra Piersigilli, Laure Menin, Alan W. Walker, Jacques Rougemont, Oonagh Paerewijck, Peter Geldhof, Kathleen D. McCoy, Andrew Macpherson, John Croese, Paul R. Giacomin, Alex Loukas, Tobias Junt, Benjamin J. Marsland, and Nicola L. Harris

Supplemental Data

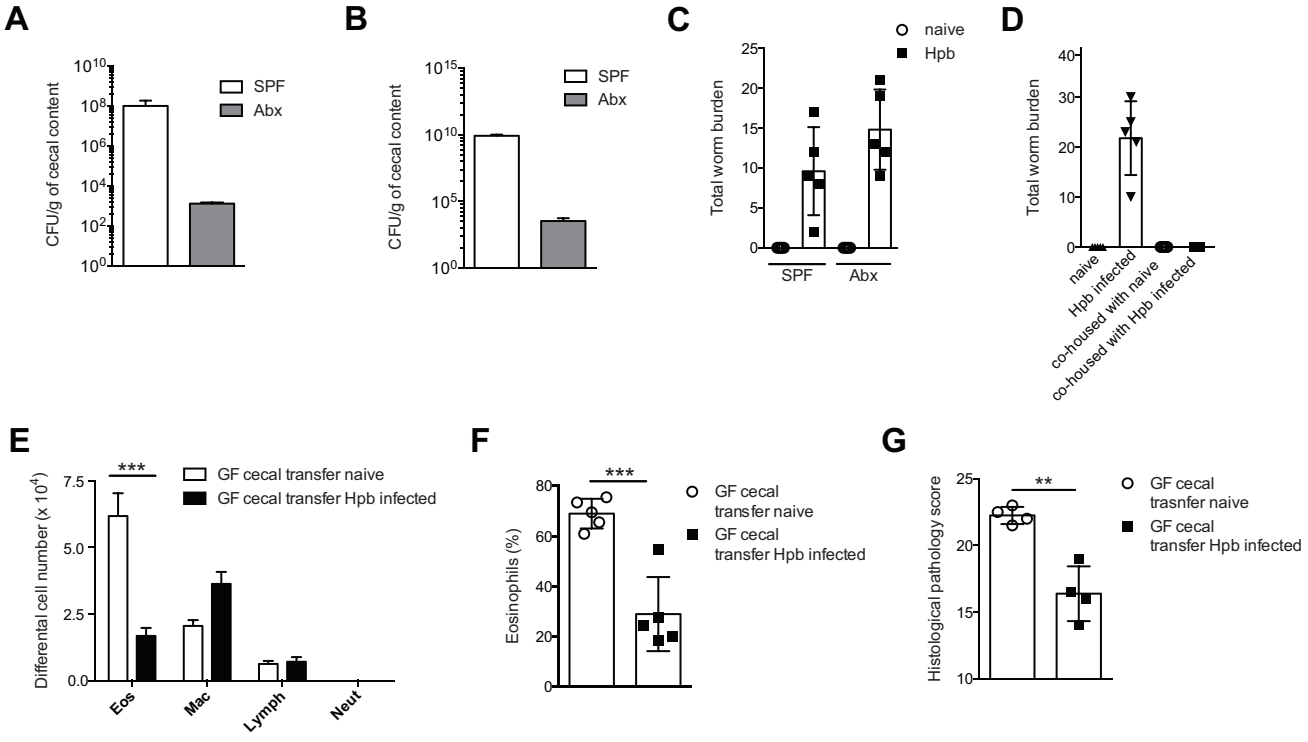

Figure S1 (related to Figure 2). Intestinal microbiota contributes to the ability of Hpb to modulate HDM-induced airway inflammation. (A-C) SPF mice were treated or not with antibiotics (Abx) and the number of (A) aerobic and (B) anaerobic colony forming units (CFUs) in cecal contents determined by bacterial plating. (C) Mice were additionally infected with Hpb and the number of adult worms in the intestine determined after 40 days. (D) Mice pretreated with antibiotics were co-housed with naive or Hpb infected SPF donors and the number of adult Hpb recovered from the intestine determined. The number of worms in both donor and recipient mice are shown. (E-G) Germ-free recipient mice were re-colonized by oral gavage with cecal contents from naive or Hpb infected donor mice. Recipients were subsequently sensitized and challenged with HDM and the ensuing allergic response determined. (E) Total differential cell counts in the BALF. (F) Percent eosinophils in BALF cells. (G) Mean gross lung histological pathology scores of H&E stained lung tissue after HDM challenges. All data are expressed as the mean +/- s.d. (n=5). Statistical significance was determined with two-way analysis of variance (ANOVA) and Student's t test. *p=0-05, **p=0-01, ***p=0.0001. Data from (A-B) are pooled from three experiments. Remaining data are from one experiment and are representative of three (C-D) or two (E-G) independent experiments.

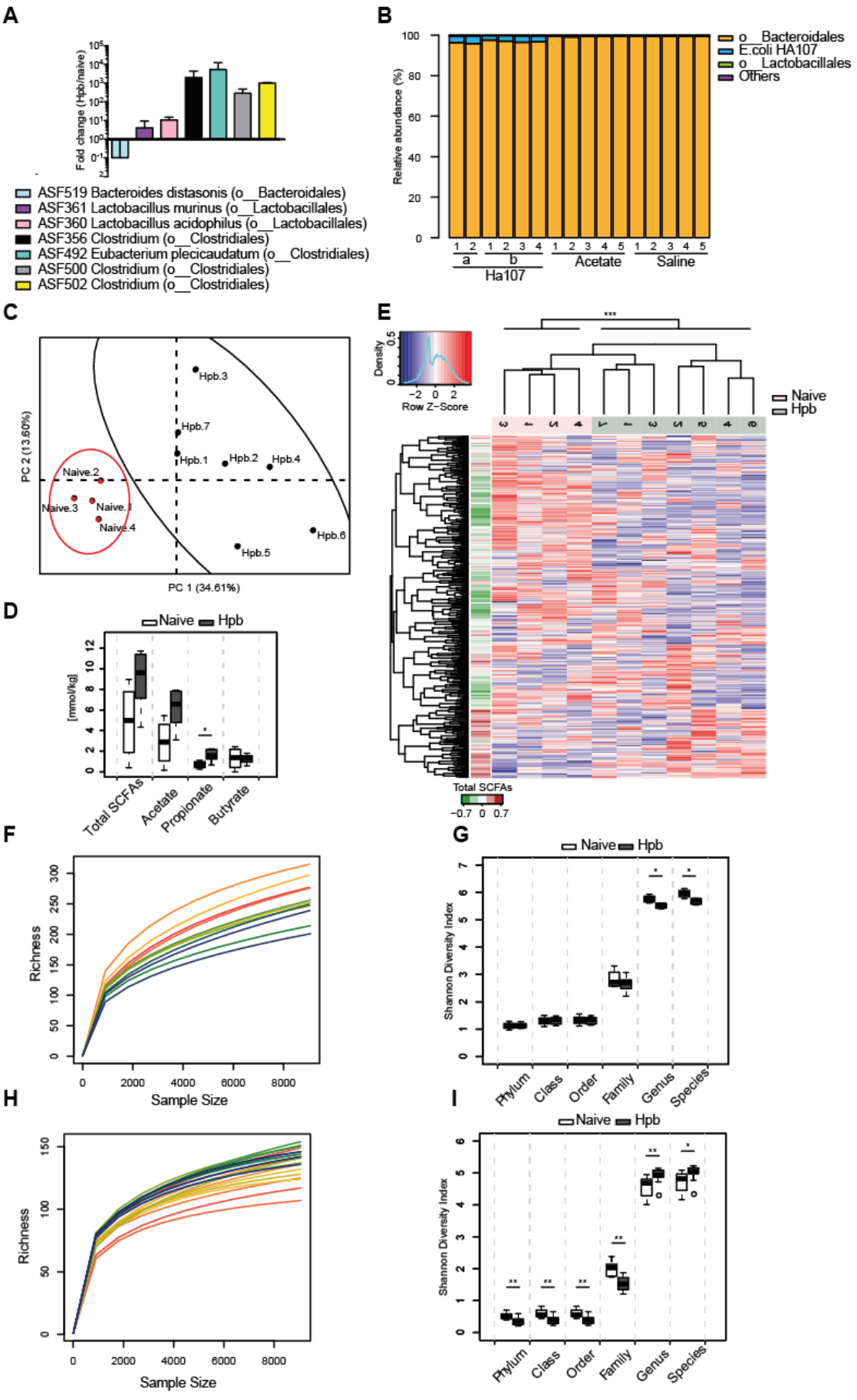
A
Fold change (Hpb/naive)
ASF519 Bacteroides distasonis (o__Bacteroidales)
ASF361 Lactobacillus murinus (o__Lactobacillales)
ASF360 Lactobacillus acidophilus (o__Lactobacillales)
ASF356 Clostridium (o__Clostridiales)
ASF492 Eubacterium plecicaudatum (o__Clostridiales)
ASF500 Clostridium (o__Clostridiales)
ASF502 Clostridium (o__Clostridiales)
B
Relative abundance (%)
o__Bacteroidales
E.coli HA107
o__Lactobacillales
Others
a
b
Ha107
Acetate
Saline
C
PC 2 (13.60%)
PC 1 (34.61%)
Hpb.3
Hpb.7
Hpb.1
Hpb.2
Hpb.4
Hpb.6
Hpb.5
Naive.2
Naive.3
Naive.1
Naive.4
D
Naive
Hpb
[mmol/kg]
Total SCFAs
Acetate
Propionate
Butyrate
E
Density
Row Z-Score
Naive
Hpb
Total SCFAs
F
Richness
Sample Size
G
Naive
Hpb
Shannon Diversity Index
Phylum
Class
Order
Family
Genus
Species
H
Richness
Sample Size
I
Naive
Hpb
Shannon Diversity Index
Phylum
Class
Order
Family
Genus
Species

Figure S2 (related to Figure 3). Hpb infection alters the cecal microbiota and increases SCFA concentrations (A) ASF mice were infected with Hpb and cecal content collected at 28 days post-infection. Data shows quantitation of ASF strains by qRT-PCR using specific primers. (B) ASF mice either received (a) $2.86x10^9$ CFU or (b) $2.15x10^3$ CFU of *E. coli* HA107 by oral gavage four weeks prior sacrifice and cecal content collection or were supplemented with 150 mM sodium acetate or 150 mM NaCl in drinking water for four weeks prior sacrifice and cecal content collection. Bacterial community composition as assessed by 16s rRNA gene sequencing is shown at the order level. (C-G) Cecal contents were collected from naive or day 40 Hpb infected SPF mice and the bacterial community was analyzed using the 16S rRNA gene sequencing method. (C) Principal coordinates analysis (PCoA) using the Bray-Curtis dissimilarity based on OTU abundances. Color clustering is based on the k-means method. Data shows individual mice. Cecal contents were collected and bacterial community was analyzed using the 16S rRNA sequencing method. (D) Cecal SCFA levels from (C). Significance determined by unpaired Student test. (E) OTU abundance heatmap from (C). The left color bar represents the Spearman correlation coefficient of each OTU with the total cecal SCFAs level. Hierarchical clustering based on the Spearman correlation coefficient was applied to order samples and OTUs. Significance determined by the Adonis method. (F) Rarefaction curves for the species richness from (C). (G) Diversity profile at multiple taxonomic levels assessed by the Shannon diversity index. (H-I) Rarefaction curves and Shannon diversity index for OTUs shown in the main Figure 3 C-E. For all data significance was determined with the Wilcoxon rank-sum test, (* $p<0.05$, ** $p<0.01$, *** $p<0.001$). Data in (A) are expressed as the mean $\pm$ s.d. (n=4-5). Data in (D, G and I) were generated using R boxplot with the middle bar representing the median and whiskers showing 1.5x Inter Quartile Range (IQR). Data are from one experiment and are representative of one (B-I) or two (A) independent experiments.

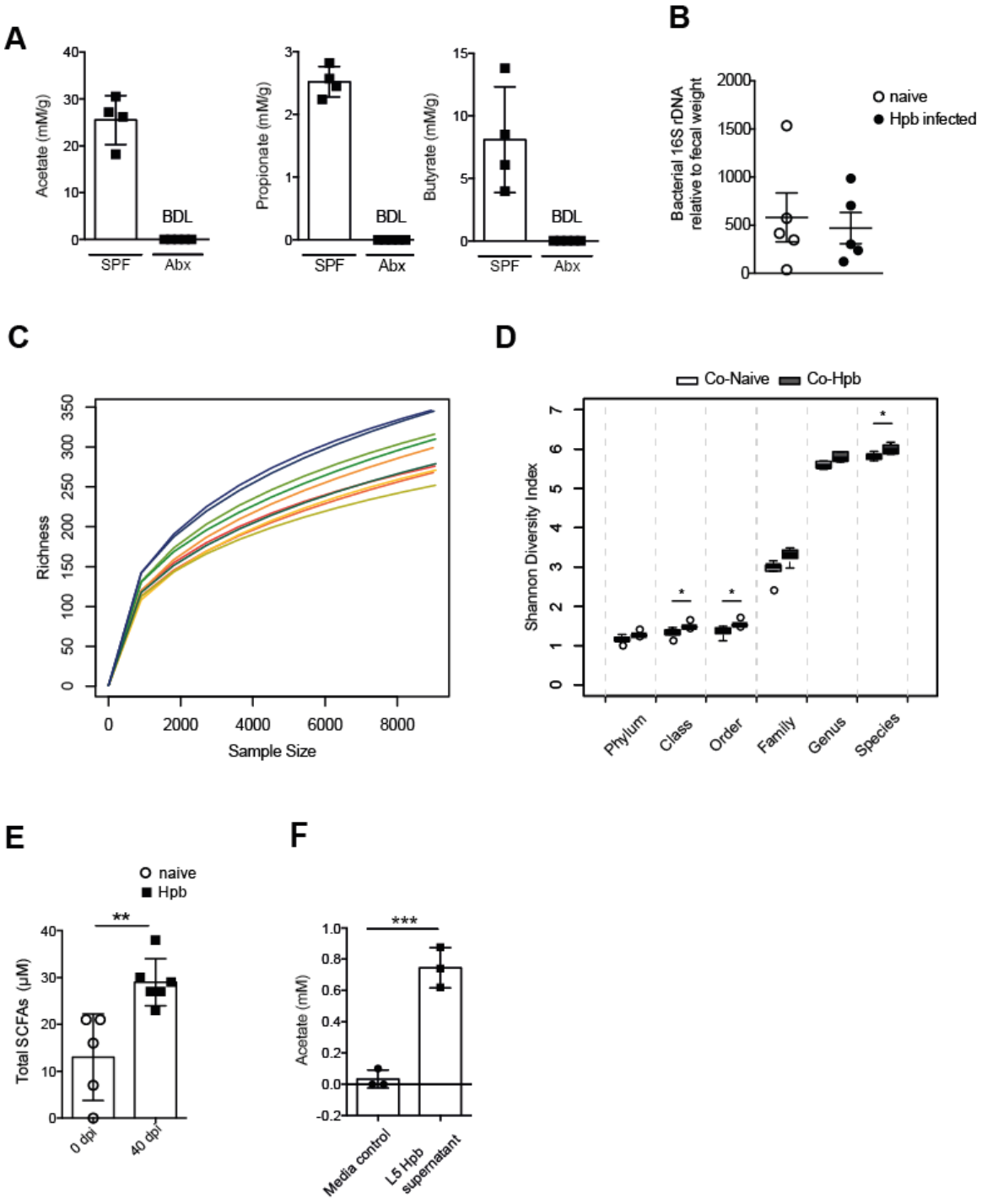
A
Acetate (mM/g)
Propionate (mM/g)
Butyrate (mM/g)
BDL
SPF
Abx
B
Bacterial 16S rDNA relative to fecal weight
naive
Hpb infected
C
Richness
Sample Size
D
Co-Naive
Co-Hpb
Shannon Diversity Index
Phylum
Class
Order
Family
Genus
Species
E
naive
Hpb
Total SCFAs (μM)
0 dpi
40 dpi
F
Acetate (mM)
Media control
L5 Hpb supernatant

Figure S3 (related to Figure 4). Hpb-induced increases in SCFA concentrations require intestinal microbial communities. (A) GC-MS quantification of SCFA acetate, propionate and butyrate levels in cecal contents of SPF and antibiotic treated (Abx) mice 40 days after infection with Hpb infective larvae. (B) RT-PCR analysis of total bacterial 16S rDNA in naive and day 40 Hpb infected mice. (C-D) Antibiotic treated recipient mice were co-housed for 3 weeks with naive SPF or Hpb infected mice and cecal contents collected and bacterial community analyzed using the 16S rRNA gene sequencing method using the same mice as depicted in Figure 4. (C) Rarefaction curves for the species richness and (D) diversity profile at multiple taxonomic levels as assessed by the Shannon diversity index. (E) GC-MS quantification of SCFA levels in the portal blood of day 40 Hpb infected and naive mice, or (F) acetate levels in in vitro cultures of adult Hpb worms. Results in (A, B, E and F) are expressed as the mean ± s.d. and statistical significance was determined with Student's t test, (* $p<0.05$, **$p<0.01$,*** $p<0.001$). For (D) data were generated using R boxplot with the middle bar representing the median and whiskers showing 1.5x Inter Quartile Range (IQR). Significance was determined with the Wilcoxon rank-sum test, (* $p<0.05$, ** $p<0.01$,*** $p<0.001$).

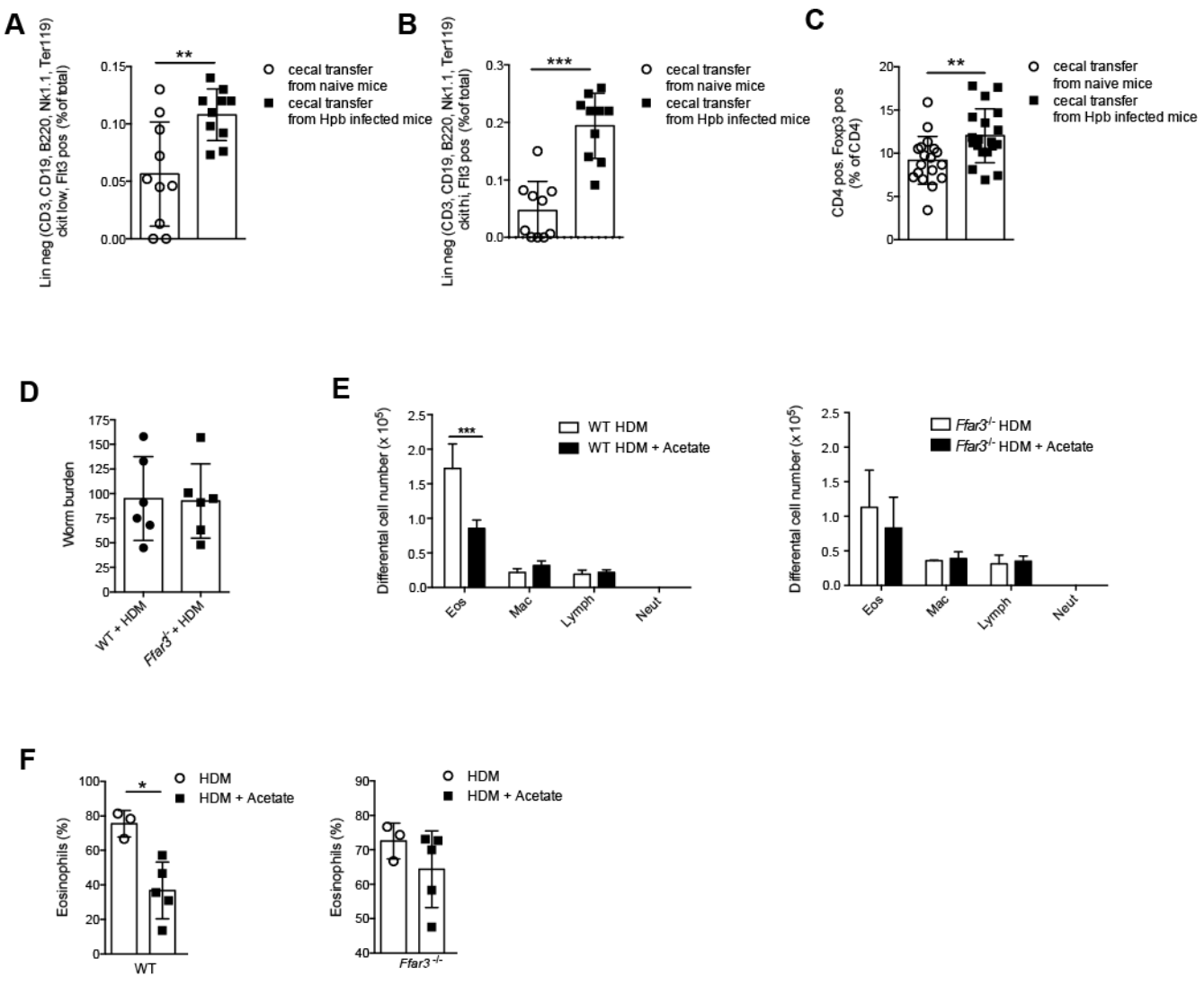

Figure S4 (related to Figure 5). SCFA-mediated attenuation of allergic airway inflammation is abrogated in *Ffar3* deficient mice. (A-C) Germ-free or antibiotic treated recipient mice were re-colonized by oral gavage of cecal contents from Hpb-infected or naive mice and 3 weeks later recipients were sensitized and challenged with HDM. Flow cytometery was used to determine the percentage of (A) common DC precursors (CDPs) and (B) macrophage and DC precursors (MDPs) in the bone marrow one day after the final HDM challenge or (C) T regs present in the lung 3 days after the final HDM challenge. (D) Wildtype or *Ffar3* deficient mice were infected with Hpb and subjected to HDM sensitization and challenge as depicted in Figure 5, and adult worms present in the intestinal lumen counted three days after the final HDM challenge. (E-F) Wildtype or *Ffar3* deficient mice were supplemented with 150 mM sodium acetate in the drinking water for four weeks then additionally subjected to HDM sensitization and challenge and BALF collected three days after the final HDM challenge. (E) Differential cell counts. Mac, macrophages; neut, neutrophils; eos, eosinophils; lymph, lymphocytes. (F) Percent eosinophils. Data in (A&B) are pooled from 2 independent experiments and data in (C) are pooled from 3 independent experiments. Data are expressed as mean ± s.d. and statistical significance determined with a Student's t test, (* $p<0.05$, ** $p<0.01$,*** $p<0.001$).

Table S1 (related to Figures 1, 2 and 5): Histological criteria for severity scoring of allergic airway inflammation.

Vasculature:

Severity	Perivascular and peribronchial/olar inflammation	Vascular hypertrophy and hyperplasia	Thickening of alveolar septa	Score (pts)
minimal	Single scattered leukocytes	Minimal thickening of the intima or media	Slightly increased cellularity	1
mild	Aggregates less than 10 cells thick	Thickening without narrowing	Alveolar wall lined by an almost continuous layer of cells	2
moderate	Aggregates about 10 cells thick	Thickening with narrowing of the lumen	Alveolar wall lined by a continuous layer of cells	3
severe	numerous coalescing aggregates more than 10 cells thick	Thickening with complete obliteration of the lumen with/without thromboemboli	Consolidation	4

Airways:

Leukocytes in alveolar spaces	Score
Absent	0
Rare cells (2-4 in 400X HPF)	1
Between 4 and 10 cells	2
More than 10 cells	3

Table S2 (related to Figures 3 and 4): Primer details used for bacterial 16S rRNA gene sequencing

	Reverse primers
	5'CAAGCAGAAGACGGCATACGAGATNNNNNNNNNNNN*AGTCAGTCAGAA***GCTGCCTCCCGTAGGAGT**3'**
	Forward primer
	5'AATGATACGGCGACCACCGAGATCTACAC*TATGGTAATTCC***AGMGTTYGATYMTGGCTCAG**3'**
	Sequencing primers
R1	5'GAGATCTACAC*TATGGTAATTCC***AGMGTTYGATYMTGGCTCAG**3'**
Index	5'**ACTCCTACGGGAGGCAGC***TTCTGACTGACT***3'
R2	5'*AGTCAGTCAGAA***GCTGCCTCCCGTAGGAGT**3'**
	Bold characters: bacteria specific 16S rRNA universal sequence F27 (forward) and R338 (reverse); Italic characters: primer pad; Italic and underlined characters: linker; Underlined characters: MID tag sequence; Thin characters: Illumina adapter.

Supplemental Experimental Procedures

Measurement of short-chain fatty acids (SCFAs)

For human SCFA analysis, frozen fecal samples were weighed into a 2 ml extraction tube. The tubes were kept in a cool rack throughout the extraction. 20 µl of internal standard (80 mM of 2-ethylbutyric acid in water, Sigma) and 200 µl of 3.2% HCl was added and samples vortexed for 1 min. 1 ml of diethyl ether was added, vortexed for 1 min and centrifuged for 3 min at 0 °C. The organic phase was transferred into a 2 ml gas chromatography (GC) vial. For the calibration curve, 100 µl of SCFA calibration standards were dissolved in water (Sigma) to concentrations of 0, 0.5, 1, 5 and 10 mM and then subjected to the same extraction procedure as the samples ($r^2 > 0.999$). All samples were run on a 7890A GC coupled to a 5975C MSD (Agilent, Palo Alto) set up with a DB-Wax, 30 m x 0.2599 x 0.2599 capillary column (Agilent). The carrier gas was helium and the column flow was 1 ml/min. The injector was set to 250 °C and the transfer line, mass spectrometry (MS) source and MS quad to 280 °C, 230 °C and 150 °C, respectively. The oven program was as follows, 50 °C initial for 1 min, then 25 °C/min to 230 °C for 10 min, with a total run time of 18 min. 1 µl of sample was injected with a split ratio of 50:1.

For mouse and pig SCFA analysis, the samples were derivatized prior to GC-MS analyses using MTBSTFA + 1 % TBDMCS as silylation reagent (Thermo Scientific). 60 µl of samples (in duplicate) were incubated with 20 µl of reagent for 1 hour at room temperature. For the calibration curve, 60 µl of the SCFA standards (acetate, propionate and butyrate) were dissolved in acetonitrile (Thermofischer) and derivatized by addition of 20 µl of reagent for 1 hour at room temperature. All samples were run on

a CP-3800 Gas Chromatograph coupled to a 1200L Quadrupole MS/MS (Varian) using a FactorFour VF-50ms, 30m x 0.25mm x 0.25mm capillary column (Varian). The carrier gas was helium and the column flow was 1 ml/min. The injector, transfer line and MS source were set to 250 °C, 250 °C and 200 °C, respectively. The oven program was as follows, 50 °C initial for 2 min, then 20 °C/min to 150 °C for 5 min, then 30 °C/min to 250 °C for 5 min. 2 µl of sample was injected and GC-MS analyses performed in duplicates. Full scan mass spectra were recorded in the 50-450 *m/z* range (1s/scan). Quantification was done by integration of the extracted ion chromatogram peaks following ion species: *m/z* 117 and 75 for acetate eluted at 5.2 min, *m/z* 131 and 75 for propionate eluted at 6.2 min, and *m/z* 145 and 75 for butyrate eluted at 6.9 min.

Bacteria quantification

Quantitative polymerase chain reaction (PCR) was performed using SYBR Green I Master Mix (Eurogentec) on a 7900HT PCR system (Applied Biosystems). Bacterial 16S rDNA and mouse 18S rDNA were amplified from total DNA using universal bacteria (Bouskra et al., 2008) and mouse-specific primers (Arizon et al., 2012). Altered Schaedler flora (ASF) species were amplified using specific primers previously described (Sarma-Rupavtarm et al., 2004).

Histology and pathology

The histopathological scoring included severity and distribution of perivascular and peribronchial/peribronchiolar inflammatory infiltrate, thickening of the alveolar septa, leukocytes in alveolar spaces as well as vascular hypertrophy and hyperplasia as detailed in Table S1. A semi-quantitative assessment of the predominant leukocyte types (eosinophils, lymphocytes, plasma cells, macrophages, etc.) in the inflammatory aggregates was also performed. The presence or absence of mucous plugs within the lumen of the bronchi and bronchiole was respectively scored with 1 and 0. The distribution of each lesion was quantified with points as follows: focal 1, multifocal 2, diffuse 3. The criteria for severity scoring of changes in the airways and vasculature are shown in Table S1. For intermediate grades of severity (such as mild to moderate, moderate to severe, etc.), 0.5 points were added to the lowest score. The total score of pulmonary damage was obtained by the sum of the single scores and is termed ‘histological pathology score’. Emphysema, atelectasis and edema were not quantified as similar changes (artifacts) were produced during the bronchoalveolar lavage. For sections stained with periodic acid-Schiff (PAS), each animal was represented by sections of the lung and five randomly selected regions from one section were evaluated (two segments of the primary conducting

airway, two segments from separate secondary conducting airways, and one segment from a tertiary conducting airway). A minimum of 100 sequential airway epithelial cells were counted from each region and the total number of PAS-positive cells per total epithelial cells was determined for each region. These regional values were then averaged to give a final PAS score per animal termed 'mean goblet cell index' (Zeki et al., 2010).

16S rRNA preparation and sequencing

DNA was first extracted from cecal content using the PowerSoil DNA isolation kit (Mo Bio Laboratories) according to manufacturer's instructions. Bacterial 16S rRNA gene V1-V2 variable regions were amplified by PCR using bar-coded primers described in Table S2 and Q5 High-fidelity PCR kit (New England Biolabs). 20 PCR cycles were performed with a template DNA input of 5 µl per 50 µl reaction mix (< 1000 ng). The temperature cycles were set as follows: 2 minutes of initial denaturing step at 98 °C, repeated steps of 30 seconds denaturing at 98 °C, 30 seconds annealing at 50 °C, 1.5 minute extension at 72 °C and a final step of 5 minutes at 72 °C. Amplicon purification was performed using the Wizard SV Gel and PCR Clean-Up System (Promega) according to manufacturer's instructions. Sequencing was performed on an Illumina MiSeq platform using MiSeq Reagent Kit v2-500 (paired-end, 2x250) with custom primers (shown in Table S2).

16S rRNA gene sequencing data analysis

Data analysis was performed using the Quantitative Insights Into Microbial Ecology (QIIME, v1.8.0) software package (Caporaso et al., 2010b) first with a closed reference OTU picking strategy, then with an open reference OTU picking strategy. Figures and statistics were generated with R (R Foundation for Statistical computing).

Low quality (< Q20) bases were truncated using Seqtk and paired end reads were merged using Fastq-join. Further quality filtering was applied and sequences were demultiplexed. Operational taxonomic units (OTUs) were picked by mapping sequences (97% similarity threshold) against a subset of the GreenGene (v13.8) sequences database filtered at 97% identity using Uclust (Haas et al., 2011). Remaining sequences were either discarded (closed reference OTU picking strategy) or clustered de-novo (open reference OTU picking strategy). Taxonomy was assigned using a pre-computed taxonomy map (closed reference OTU picking strategy) or using the Ribosomal Database Project (RDP) classifier (open reference OTU picking strategy) (Wang et al., 2007).

Starting with a closed reference OTU picking strategy, OTU tables from each experiment were

analyzed separately. OTU tables were first normalized using the rarefaction method at a depth of 9090 and calculating an average table from five random sampling repeats. OTUs representing less than 0.006% of the counts in at least one sample and present in less than 40% of the samples were discarded. Separate OTU tables were then generated for the phylum, class, order, family, genus and species (OTU) levels. Diversity was analyzed by assessing the Shannon index at multiple taxonomic levels and the richness at multiple rarefaction depths. Statistical significance was determined by Wilcoxon rank-sum test. The variance-stabilizing transformation (VST) as implemented in DESeq (Anders and Huber, 2010) was applied before comparison of experimental groups based on OTU abundances: a principal coordinates analysis (PCoA) was done using the Bray-Curtis dissimilarity based on OTU abundances and samples were clustered using the k-means method. A heat map was built based on centered and scaled OTU abundances. Samples and OTUs were ordered by hierarchical clustering using hclust based on the Spearman correlation coefficient matrix and statistical significance was determined using the permutational multivariate analysis of variance using distance matrices (Adonis method). A color bar representing the Spearman correlation coefficient of each individual OTU with SCFA levels was added.

To perform an in-depth analysis of commonalities between independent experiments, OTUs tables were generated together for all experiments using an open OTU picking strategy. To improve the taxonomic classification of OTUs assigned to poorly characterized yet relatively abundant bacterial families (Lachnospiraceae, Ruminococcaceae and S24-7), representative sequences for these families were used to build a phylogenetic tree using PyNAST (Caporaso et al., 2010a) and FastTree (Price et al., 2010) and new OTUs clusters within these families were defined based on the patristic distance and added to the original OTU taxonomy. OTU tables were then normalized using the rarefaction method at a depth of 10800 and calculating an average table from five random sampling repeats. OTUs representing less than 0.006% of the counts in at least one sample and present in less than 40% of the samples were discarded. The variance-stabilizing transformation as implemented in DESeq (Anders and Huber, 2010) was applied before comparison of experimental groups based on OTUs abundances. In each experiment, OTUs were tested for group differences by Wilcoxon rank-sum test. To highlight commonalities between experiments, OTUs showing a common fold change sign across all experiments and a significant change in at least one experiment (adjusted p-value < 0.05) were selected.

Supplemental References

Anders, S., and Huber, W. (2010). Differential expression analysis for sequence count data. Genome Biology *11*.

Arizon, M., Nudel, I., Segev, H., Mizraji, G., Elnekave, M., Furmanov, K., Eli-Berchoer, L., Clausen, B.E., Shapira, L., and Wilensky, A. (2012). Langerhans cells down-regulate inflammation-driven alveolar bone loss. Proceedings of the National Academy of Sciences *109*, 7043-7048.

Bouskra, D., Brézillon, C., Bérard, M., Werts, C., Varona, R., Boneca, I.G., and Eberl, G. (2008). Lymphoid tissue genesis induced by commensals through NOD1 regulates intestinal homeostasis. Nature *456*, 507-510.

Caporaso, J.G., Bittinger, K., and Bushman, F.D. (2010a). PyNAST: a flexible tool for aligning sequences to a template alignment. Bioinformatics *26*, 266-267.

Caporaso, J.G., Kuczynski, J., Stombaugh, J., and Bittinger, K. (2010b). QIIME allows analysis of high-throughput community sequencing data. Nature Methods *7*.

Haas, B.J., Gevers, D., Earl, A.M., and Feldgarden, M. (2011). Chimeric 16S rRNA sequence formation and detection in Sanger and 454-pyrosequenced PCR amplicons. Genome Research *21*, 494-504.

Price, M.N., Dehal, P.S., and Arkin, A.P. (2010). FastTree 2–approximately maximum-likelihood trees for large alignments. PloS One *5*.

Sarma-Rupavtarm, R.B., Ge, Z., Schauer, D.B., Fox, J.G., and Polz, M.F. (2004). Spatial distribution and stability of the eight microbial species of the altered schaedler flora in the mouse gastrointestinal tract. Applied and Environmental Microbiology *70*, 2791-2800.

Wang, Q., Garrity, G.M., and Tiedje, J.M. (2007). Naive Bayesian classifier for rapid assignment of rRNA sequences into the new bacterial taxonomy. Applied and Environmental Microbiology *73*, 5261-5267.

Zeki, A.A., Bratt, J.M., Rabowsky, M., and Last, J.A. (2010). Simvastatin inhibits goblet cell hyperplasia and lung arginase in a mouse model of allergic asthma: a novel treatment for airway remodeling? Translational Research *156*, 335-349.